

Cost Effective Optimization for Cost-related Hyperparameters

Qingyun Wu^{1*} Chi Wang² Silu Huang²

Abstract

The increasing demand for democratizing machine learning algorithms for general software developers calls for hyperparameter optimization (HPO) solutions at low cost. Many machine learning algorithms have hyperparameters, which can cause a large variation in the training cost. But this effect is largely ignored in existing HPO methods, which are incapable to properly control cost during the optimization process. To address this problem, we develop a cost effective HPO solution. The core of our solution is a new randomized direct-search method. We prove a convergence rate of $O(\frac{\sqrt{d}}{\sqrt{K}})$ and provide an analysis on how it can be used to control evaluation cost under reasonable assumptions. Extensive evaluation using a latest AutoML benchmark shows a strong any time performance of the proposed HPO method when tuning cost-related hyperparameters.

1. Introduction

Machine learning algorithms usually involve a number of hyperparameters that have a large impact on model accuracy and need to be set appropriately for each task. For developers to easily use ML algorithms and confidently deploy them in software, there needs to be an efficient method to automatically tune these hyperparameters at low cost. It motivates research in cost-effective hyperparameter optimization (HPO).

While HPO is mostly considered as a black-box function optimization problem, machine learning algorithms are black-box functions with high evaluation cost since training a model can be time-consuming. So the cost of function evaluation is an important factor in the overall optimization cost. Further, this cost can be directly affected by a subset of hyperparameters. For example, in gradient boosted trees, the variation of the number of trees and the depth per tree

can result in a large variation on training and validation time. Unfortunately, this correlation is ignored by most existing HPO methods. That makes them not optimized for the overall cost because they may waste time on evaluating hyperparameters corresponding to high cost. For example, the dominating search strategy Bayesian optimization (Brochu et al., 2010; Bull, 2011) methods are designed for minimizing the total number of function evaluations, which does not necessarily lead to low evaluation cost. There exists some heuristic technique to model the evaluation cost using another probabilistic model (Snoek et al., 2012), but it does not prevent unnecessarily expensive evaluations before the probabilistic model collects many evaluation results. More recent work controls cost in HPO by using multi-fidelity optimization, such as BOCA (Kandasamy et al., 2017), FABOLAS (Klein et al., 2017), Hyperband (Li et al., 2017) and BOHB (Falkner et al., 2018). They assume the optimal configuration corresponds to maximal fidelity or budget, so the notion of fidelity or budget is not suitable for modeling generic cost-related hyperparameters.

In this paper, we take a fresh and unique path of addressing HPO based on *randomized direct-search*, and develop a cost-effective optimization method CEO. Our solution is designed toward both small number of iterations before convergence and bounded cost per iteration, which lead to low total evaluation cost.

Specifically, CEO is built upon our newly proposed randomized direct search method FLOW², which has a mixed flavor of zeroth-order optimization (Nesterov & Spokoiny, 2017) and directional direct search (Kolda et al., 2003). First, we prove that FLOW² enjoys a convergence rate of $O(\frac{\sqrt{d}}{\sqrt{K}})$ even in the non-convex case under a common smoothness condition. This convergence result is of independent interest in the theory of derivative-free optimization. Second, we prove that due to FLOW²'s unique update rule, when it is combined with a low-cost initialization, the cost in any iteration of FLOW² can be upper bounded under reasonable conditions. Combining these two results, we prove that the total cost for obtaining an ϵ -approximation of the loss is bounded by $O(de^{-2})$ times the optimal configuration's cost by expectation. We also prove that when the computational complexity of the ML algorithm with respect to the hyperparameters is known, with a proper transformation on the original value of the optimization variables, the total cost

*The work is done when the author was at Microsoft Research
¹ University of Virginia, Charlottesville, VA, USA ²Microsoft Research, Redmond, WA, USA. Correspondence to: Qingyun Wu <qw2ky@virginia.edu>.

bound can be further reduced. To the best of our knowledge, such theoretical bound on cost does not exist in any HPO literature. Also, we incorporate several practical adjustments, including adaptive step size and random restart, etc., on top of FLOW² and build a practical off-the-shelf HPO solution CEO.

We perform extensive evaluations using a latest AutoML benchmark (Gijsbers et al., 2019) which contains large scale classification tasks. We also enrich it with datasets from a regression benchmark (Olson et al., 2017) to test regression tasks. Comparing to random search and three variations of Bayesian optimization, CEO shows better anytime performance and better final performance in tuning a popular library XGBoost (Chen & Guestrin, 2016) and neural network model on most of the tasks with a significant margin within the given time budget.

2. Related Work

The most straightforward HPO method is grid search. Grid search discretizes the search space of the concerned hyperparameters and tries all the values in the grid. The number of function evaluations in grid search increases exponentially with hyperparameter dimensions. A simple yet surprisingly effective alternative is to use random combinations of hyperparameter values, especially when the objective function has a low effective dimensionality, as shown in (Bergstra & Bengio, 2012). The most dominating search strategy for HPO is Bayesian optimization (BO) (Brochu et al., 2010). Bayesian optimization uses a probabilistic model to approximate the blackbox function to optimize. When performing Bayesian optimization, one needs to make two major choices. First, one needs to select a prior over functions that will express assumptions about the function being optimized. For example, Snoek et al. (Snoek et al., 2012) uses Gaussian process (GP), Bergstra et al. (Bergstra et al., 2011) uses the tree Parzen estimator (TPE), and Hutter et al. (Hutter et al., 2011) uses random forest (SMAC). Second, one needs to choose an acquisition function, which is used to construct a utility function from the model posterior, allowing us to determine the next point to evaluate. Two common acquisition functions are the *expected improvement* (EI) over the currently best observed value, and *upper confidence bound* (UCB).

Some recent work studies ways to control cost in HPO using multi-fidelity optimization. FABOLAS (Klein et al., 2017) introduces dataset size as an additional degree of freedom in Bayesian optimization. Hyperband (Li et al., 2017) and BOHB (Falkner et al., 2018) try to reduce cost by allocating gradually increasing ‘budgets’ to a number of evaluations at different stages of the search process. The notion of budget can correspond to either sample size or the number of iterations for iterative training algorithms. These solutions assume the evaluation cost to be equal or similar

for each fixed ‘budget’, which is not necessarily true when the hyperparameters to tune can greatly affect evaluation cost. These solutions also require a predefined ‘maximal budget’ and assume the optimal configuration is found at the maximal budget. So the notion of budget is not suitable for modeling even a single cost-related hyperparameter whose optimal value is not necessarily at maximum, e.g., the number K in K-nearest-neighbor algorithm. The same is true for two other multi-fidelity methods BOCA (Kandasamy et al., 2017) and BHPT (Lu et al., 2019).

3. Cost Effective Hyperparameter Optimization

In the rest of this section, we will present (1) the problem setup of cost-effective optimization; (2) a new randomized direct search method FLOW²; (3) an analysis on the convergence of FLOW²; (4) an analysis on the evaluation cost of FLOW²; (5) a cost effective HPO method CEO, which is built upon FLOW².

3.1. Problem setup

Denote $f(\mathbf{x})$ as a black-box loss function of $\mathbf{x} \in \mathcal{X} \subset \mathbb{R}^d$. In the HPO scenario, it can be considered as the loss on the validation dataset of the concerned machine learning algorithm, which is trained on the given training dataset using hyperparameter \mathbf{x} . In HPO, each function evaluation on \mathbf{x} invokes an evaluation cost of $g(\mathbf{x})$, which can have large variation with respect to a subset of dimensions of \mathbf{x} . In most real-world scenarios where HPO is needed, evaluation cost is preferred to be small. In this paper, we target at minimizing $f(\mathbf{x})$ while preferring small $\sum_{i=1}^{k^*} g(\mathbf{x}_i)$, where k^* is the number of function evaluations involved when the minimum value of $f(\mathbf{x})$ is found. Apparently, no solution can be better than directly evaluating the optimal configuration \mathbf{x}^* , which has the lowest loss $f(\mathbf{x}^*)$ and lowest total evaluation cost $g(\mathbf{x}^*)$ among all the minimizers of f . Our goal is to use minimal cost to approach $f(\mathbf{x}^*)$. Then the problem to solve can be rewritten as: $\min_{\mathbf{x} \in \mathcal{X}} f(\mathbf{x})$ with preference to small $\sum_{i=1}^{k^*} g(\mathbf{x})$.

3.2. FLOW²

Our algorithm FLOW² is presented in Algorithm 1. At each iteration k , we sample a vector \mathbf{u}_k uniformly at random from a $(d-1)$ -unit sphere \mathbb{S} . Then we compare loss $f(\mathbf{x}_k + \delta \mathbf{u}_k)$ and $f(\mathbf{x}_k)$, if $f(\mathbf{x}_k + \delta \mathbf{u}_k) < f(\mathbf{x}_k)$, then \mathbf{x}_{k+1} is updated as $\mathbf{x}_k + \delta \mathbf{u}_k$; otherwise we compare $f(\mathbf{x}_k - \delta \mathbf{u}_k)$ with $f(\mathbf{x}_k)$. If the loss is decreased, then \mathbf{x}_{k+1} is updated as $\mathbf{x}_k - \delta \mathbf{u}_k$, otherwise \mathbf{x}_{k+1} stays at \mathbf{x}_k . Our proposed solution is built upon the insight that if $f(\mathbf{x})$ is differentiable¹ and δ is small,

¹For non-differentiable functions we can use smoothing techniques, such as Gaussian smoothing (Nesterov & Spokoiny, 2017)

Algorithm 1 FLOW²

```

1: Inputs: Stepsize  $\delta > 0$ , initial value  $\mathbf{x}_0$ , and number
   of iterations  $K$ .
2: for  $k = 1, 2, \dots, K$  do
3:   Sample  $\mathbf{u}_k$  uniformly at random from unit sphere  $\mathbb{S}$ 
4:   if  $f(\mathbf{x}_k + \delta \mathbf{u}_k) < f(\mathbf{x}_k)$  then
5:      $\mathbf{x}_{k+1} = \mathbf{x}_k + \delta \mathbf{u}_k$ 
6:   else
7:     if  $f(\mathbf{x}_k - \delta \mathbf{u}_k) < f(\mathbf{x}_k)$  then
8:        $\mathbf{x}_{k+1} = \mathbf{x}_k - \delta \mathbf{u}_k$ 
9:     else
10:     $\mathbf{x}_{k+1} = \mathbf{x}_k$ 

```

$\frac{f(\mathbf{x} + \delta \mathbf{u}) - f(\mathbf{x})}{\delta}$ can be considered as an approximation to the directional derivative of loss function on direction \mathbf{u} , i.e., $f'_{\mathbf{u}}(\mathbf{x})$. By moving toward the directions where the approximated directional derivative $\frac{f(\mathbf{x} + \delta \mathbf{u}) - f(\mathbf{x})}{\delta} \approx f'_{\mathbf{u}}(\mathbf{x})$ is negative, it is likely that we can move toward regions that can decrease the loss.

Although FLOW² can be used to solve general black-box optimization problems, it is especially appealing for HPO scenarios where function evaluation cost is high and depends on the optimization variables. First, after each iteration \mathbf{x}_{k+1} will be updated to $\mathbf{x}_k \pm \delta \mathbf{u}_k$ or stays at \mathbf{x}_k , the function value of which has already been evaluated in line 4 or line 7. It means that only one or two new function evaluations are involved in each iteration of FLOW². Second, at every iteration, we will first check whether the proposed new points can decrease loss before updating \mathbf{x}_{k+1} . In this case, new function evaluations will only be invoked at points with bounded evaluation cost ratio with respect to the currently best point. We can prove that because of this update rule, if the starting point \mathbf{x}_0 is initialized at a low-cost region and the stepsize is properly controlled, our method can effectively avoid unnecessary high-cost evaluations that are much larger than the optimal points cost (more analysis in Section 3.4). As a downside, FLOW² is subject to converging to local optimum. We address that issue in Section 3.5.

In contrast to Bayesian optimization methods, FLOW² inherits advantages of zeroth-order optimization and directional direct search methods in terms of refraining from dramatic changes in hyperparameter values (and therefore evaluation cost). And our method overcomes some disadvantages of existing zeroth-order optimization and direct search methods in our context. For example, in the directional direct search methods (Kolda et al., 2003), a move will guarantee a decreased loss, yet the lack of randomness in the search directions makes it require trying $O(d)$ directions before each move. On the other hand, in the zeroth-order opti-

to make a close differentiable approximation of the original objective function.

mization methods (Nesterov & Spokoiny, 2017; Liu et al., 2019), only one direction is tried before each move. But \mathbf{x}_{k+1} is not set to $\mathbf{x}_k \pm \delta \mathbf{u}_k$, which means that there must be function evaluations on two new points at each iteration. And the loss does not necessarily decrease after each move.

3.3. Convergence of FLOW²

We now provide a rigorous analysis on the convergence of FLOW² in both non-convex and convex cases under a L-smoothness condition.

Assumption 1 (L-smoothness). *Differentiable function f is L-smooth if for some non-negative constant L , $\forall \mathbf{x}, \mathbf{y} \in \mathcal{X}$,*

$$|f(\mathbf{y}) - f(\mathbf{x}) - \nabla f(\mathbf{x})^T(\mathbf{y} - \mathbf{x})| \leq \frac{L}{2} \|\mathbf{y} - \mathbf{x}\|^2 \quad (1)$$

where $\nabla f(\mathbf{x})$ denotes the gradient of f at \mathbf{x} .

Proposition 1. *Under Assumption 1, FLOW² guarantees:*

$$f(\mathbf{x}_k) - \mathbb{E}_{\mathbf{u}_k \in \mathbb{S}}[f(\mathbf{x}_{k+1}) | \mathbf{x}_k] \geq \delta c_d \|\nabla f(\mathbf{x}_k)\|_2 - \frac{L\delta^2}{2} \quad (2)$$

$$\text{in which } c_d = \frac{2\Gamma(\frac{d}{2})}{(d-1)\Gamma(\frac{d-1}{2})\sqrt{\pi}}.$$

This proposition provides a lower bound on the expected decrease of loss for every iteration in FLOW², where expectation is taken over the randomly sampled directions \mathbf{u}_k . This lower bound depends on the norm of gradient and the stepsize, and sets the foundation of the convergence to a first-order stationary point (in non-convex case) or global optimum (in convex case) when stepsize δ is set properly.

Proof idea The main challenge in our proof is to properly bound the expectation of the loss decrease over the random directions \mathbf{u}_k . While \mathbf{u}_k is sampled uniformly from the unit hypersphere, the update condition (Line 4 and 7) filters these directions and complicates the computation of the expectation. Our solution is to partition the unit sphere \mathbb{S} into different regions according to the value of the directional derivative. For the regions where the directional derivative along the sampled direction \mathbf{u}_k has large absolute value, it can be shown that our moving direction is close to the gradient descent direction using the L-smoothness condition, which leads to large decrease in loss. We prove that even if the loss decrease for \mathbf{u} in other regions is 0, the overall expectation of loss decrease is close to the expectation of absolute directional derivative over the unit sphere, which is equal to $c_d \|f(\mathbf{x}_k)\|_2$ according to a technical lemma proved in this paper. The full proof is in Appendix A.

Define $\mathbf{x}^* = \arg \min_{\mathbf{x} \in \mathcal{X}} f(\mathbf{x})$ as the global optimal point.

Theorem 1 (Convergence of FLOW² in the non-convex case). *Under Assumption 1,*

$$\min_{k \in [K]} \mathbb{E}[\|\nabla f(\mathbf{x}_k)\|_2] \leq \frac{r_0 + \frac{1}{2}LK\delta^2}{c_d(K-1)\delta} \quad (3)$$

in which $\frac{1}{c_d} = O(\sqrt{d})$, and $r_0 = f(\mathbf{x}_0) - f(\mathbf{x}^*)$. By letting $\delta \propto \frac{1}{\sqrt{K}}$,

$$\min_{k \in [K]} \mathbb{E}[\|\nabla f(\mathbf{x}_k)\|_2] = O\left(\frac{\sqrt{d}}{\sqrt{K}}\right) \quad (4)$$

Theorem 1 proves the expected convergence of $f(\mathbf{x})$ to a first-order stationary point in the non-convex case. It is in general a strong enough convergence result in the non-convex case. In Section 3.5, we further discuss some practical improvements.

Theorem 2 (Convergence of FLOW² in the convex case). *If f is convex and satisfies Assumption 1,*

$$\mathbb{E}[f(\mathbf{x}_K)] - f(\mathbf{x}^*) \leq e^{-\frac{\delta c_d K}{R}} r_0 + \frac{L\delta R}{2c_d} \quad (5)$$

in which c_d is defined as in Proposition 1, $r_0 = f(\mathbf{x}_0) - f(\mathbf{x}^*)$ and $R = \max_{k \in [K]} \|\mathbf{x}_k - \mathbf{x}^*\|_2$. If $\delta \propto \frac{1}{\sqrt{K}}$,

$$\mathbb{E}[f(\mathbf{x}_K)] - f(\mathbf{x}^*) \leq e^{-\frac{c_d \sqrt{K}}{R}} r_0 + \frac{LR}{2c_d \sqrt{K}} \quad (6)$$

The proof of Theorem 1 and Theorem 2 can be derived based on the conclusion in Proposition 1. Details of the proofs can be found in Appendix A.

The convergence results in Theorem 1 and Theorem 2 show that FLOW² can achieve a convergence rate of $O(\frac{\sqrt{d}}{\sqrt{K}})$ in both non-convex and convex case when $\delta \propto \frac{1}{\sqrt{K}}$. The best convergence rate so far for zeroth-order optimization methods that only use function evaluations is $O(\frac{d}{K})$ (Nesterov & Spokoiny, 2017). It has better dependency on K but worse dependency on d . And that convergence rate requires step-size to be dependent on extra unknowns besides the total number of iterations, which makes it hard to achieve in practice. The best known convergence result for the commonly used Bayesian optimization methods in HPO problems is $O(K^{-v/d})$, which is derived for BO with Gaussian process model and expected improvement acquisition function (Bull, 2011). It requires a Gaussian prior with a smoothness parameter v . The comparison between our convergence result and their convergence result with respect to K depends on the smoothness parameter v of the Gaussian prior. When $v < 2d$, our result has a better dependency on K . And our convergence result has a better dependency on d .

3.4. Cost analysis of FLOW²

In this section, we provide a rigorous analysis of the cost behavior of FLOW². We first provide an analysis in a more general case, where only two mild assumptions are needed to bound the expected total cost of FLOW². Then we show how this general case cost bound can be further reduced when the computational complexity of the ML algorithm with respect to the hyperparameters is known.

3.4.1. COST ANALYSIS IN GENERAL CASES

In this subsection, we first state two mild assumptions about the cost function, and then provide an upper bound of the cost for FLOW² when those assumptions are satisfied.

Assumption 2 (Lipschitz continuity of cost function $g(\mathbf{x})$). $\forall \mathbf{x}_1, \mathbf{x}_2 \in \mathcal{X}$,

$$|g(\mathbf{x}_1) - g(\mathbf{x}_2)| \leq U \times z(\mathbf{x}_1 - \mathbf{x}_2) \quad (7)$$

in which U is the Lipschitz constant, and $z(\mathbf{x}_1 - \mathbf{x}_2)$ is a particular function of $\mathbf{x}_1 - \mathbf{x}_2$. For example $z(\cdot)$ can be the l_2 norm function, $z(\mathbf{x}_1 - \mathbf{x}_2) = \|\mathbf{x}_1 - \mathbf{x}_2\|$.

Using the same notations as those in the above Lipschitz continuity assumption, we define $D := U \times \max_{\mathbf{u} \in \mathbb{S}} z(\delta \mathbf{u})$.

Assumption 3 (Local monotonicity between cost and loss). $\forall \mathbf{x}_1, \mathbf{x}_2 \in \mathcal{X}$, if $2D + g(\tilde{\mathbf{x}}^*) \geq g(\mathbf{x}_1) > g(\mathbf{x}_2) \geq g(\tilde{\mathbf{x}}^*)$, then $f(\mathbf{x}_1) \geq f(\mathbf{x}_2)$.

Assumption 3 assumes that when the cost surpasses a locally optimal point $\tilde{\mathbf{x}}^*$'s cost, i.e., $g(\mathbf{x}) \geq g(\tilde{\mathbf{x}}^*)$, with the increase of the evaluation cost in a local range, the loss increases. Intuitively, for most ML models, when the model's complexity is increased beyond a suitable size, the model's performance would drop while the complexity increases due to overfitting. To give a concrete example, let us consider the number K in K -nearest-neighbor. Assumption 3 essentially means that the further is K above the optimal point, the larger is the validation loss, which is typically true in the surrounding space of the optimal point.

Proposition 2 (Bounded cost change in FLOW²). *If Assumption 2 is true, then $g(\mathbf{x}_{k+1}) \leq g(\mathbf{x}_k) + D, \forall k$.*

The proof of this proposition is straightforward based on the Lipschitz continuity assumption. Intuitively this proposition is true because FLOW² is doing local search. Similar conclusion can be obtained for other local search methods under Assumption 2, but not for global optimization methods, such as Bayesian optimization.

Denote $\tilde{\mathbf{x}}^*$ as a first-order stationary point of f .

Proposition 3 (Bounded cost for any function evaluation of FLOW²). *If Assumption 2 and Assumption 3 are true, then $g(\mathbf{x}_k) \leq g(\tilde{\mathbf{x}}^*) + D, \forall k$.*

Proposition 3 asserts that the cost of each evaluation is within a constant away from the evaluation cost of the locally optimal point. The high-level idea is that FLOW² will only move when there is a decrease in the validation loss and thus the search procedure would not use much more than the locally optimal point's evaluation cost once it enters the locally monotonic area defined in Assumption 3. Unlike the previous proposition, Proposition 3 is not necessarily true for all local search methods. This appealing cost bound relies on the specially designed update rule in FLOW².

Define T as the expected total evaluation cost for FLOW² to approach a first-order stationary point $f(\tilde{\mathbf{x}}^*)$ within distance ϵ . K^* is the expected number of iterations taken by FLOW² until convergence. According to Theorem 1, $K^* = O(\frac{d}{\epsilon^2})$.

Theorem 3 (Expected total evaluation cost of FLOW²). *Under Assumption 2 and Assumption 3, if $K^* \leq \lceil \frac{\gamma}{D} \rceil$, $T \leq K^*(g(\tilde{\mathbf{x}}^*) + g(\mathbf{x}_0)) + 2K^*D$; else, $T \leq 2K^*g(\tilde{\mathbf{x}}^*) + 4K^*D - (\frac{\gamma}{D} - 1)\gamma$, in which $\gamma = g(\tilde{\mathbf{x}}^*) - g(\mathbf{x}_0) > 0$.*

Theorem 3 shows that the total evaluation cost of FLOW² depends on the number of iterations K^* , the maximal growth of cost for one iteration D , and the evaluation cost gap γ between the initial point \mathbf{x}_0 and $\tilde{\mathbf{x}}^*$. From this conclusion we can see that as long as the initial point is a low-cost point, i.e., $\gamma > 0$ the evaluation cost is always bounded by $T \leq 4K^* \cdot (g(\tilde{\mathbf{x}}^*) + g(\mathbf{x}_0) + D) = O(d\epsilon^{-2})g(\tilde{\mathbf{x}}^*)$. Notice that $g(\tilde{\mathbf{x}}^*)$ is the minimal cost to spend on evaluating the locally optimal point $\tilde{\mathbf{x}}^*$. Our result suggests that the total cost for obtaining an ϵ -approximation of the loss is bounded by $O(d\epsilon^{-2})$ times that minimal cost by expectation. When the cost function g is a constant, our result degenerates the bound on the number of iterations. To the best of our knowledge, we have not seen cost bounds of similar generality in existing work.

Proof idea We partition the iterations in FLOW² into two parts depending on whether $g(\mathbf{x}_k)$ is smaller than $g(\tilde{\mathbf{x}}^*)$. Then the upper bound of the evaluation cost over the first part of iterations is an arithmetic sequence starting from $g(\mathbf{x}_0)$ to $g(\tilde{\mathbf{x}}^*)$ with a change of D in each step. This arithmetic series ends at iteration $\bar{k} = \lceil \frac{\gamma}{D} \rceil$. Since \bar{k} -th iteration, we can upper bound each evaluation cost using $g(\tilde{\mathbf{x}}^*) + I \times \max_{\mathbf{u} \in \mathbb{S}} z(\delta\mathbf{u})$ according to Prop 3. Intuitively speaking, the expected total cost in the first part mainly depends on the gap between $g(\mathbf{x}_0)$ and $g(\tilde{\mathbf{x}}^*)$, and D . The expected total cost in the second part only increases linearly with $(K^* - \bar{k} + 1)D$. Summing these two parts up gives the conclusion.

Remark 1. *Theorem 3 holds as long as Lipschitz continuity (Assumption 2) and local monotonicity (Assumption 5) are satisfied. It does not rely on the smoothness condition. So the cost analysis has its value independent of the convergence analysis.*

3.4.2. COST ANALYSIS OF FLOW² WITH FACTORIZED FORM OF COST FUNCTION

In this section, we consider a particular form of cost function and provide the cost analysis of FLOW² with such a cost function. Specifically, we consider the type of cost which satisfies Assumption 4.

Assumption 4. *The cost function $g(\cdot)$ in terms of \mathbf{x} can be written into a factorized form $g(\mathbf{x}) = \prod_{i=1}^{d'} e^{\pm x_i}$, where $d' \leq d$ is number of dimensions where the coordinates is cost-related.*

We acknowledge that such an assumption on the function is not necessarily always true in all the cases. We will illustrate how to apply proper transformation functions on the original hyperparameter variables to realize Assumption 4 later in this subsection.

With the factorized form specified in Assumption 4, the following fact is true.

Fact 1 (Invariance of cost ratio). *If Assumption 4 is true, $\frac{g(\mathbf{x} + \Delta)}{g(\mathbf{x})} = c(\Delta)$, in which $c(\Delta) = e^{\sum_{i=1}^{d'} \pm \Delta_i}$.*

Implication of Fact 1: according to Fact 1, $\log(g(\mathbf{x}_1)) - \log(g(\mathbf{x}_2)) = \sum_{i=1}^{d'} ((\pm x_{1,i}) - (\pm x_{2,i}))$. It means that if the cost function can be written into a factorized form, the Lipschitz continuous assumption in Assumption 2 is true in the log space of the cost function.

Using the same notation as that in Fact 1, we define $C := \max_{\mathbf{u} \in \mathbb{S}} c(\delta\mathbf{u})$.

Assumption 5 (Local monotonicity between cost and loss). *$\forall \mathbf{x}_1, \mathbf{x}_2 \in \mathcal{X}$, if $\max\{2D, (C^2 - 1)g(\tilde{\mathbf{x}}^*)\} + g(\tilde{\mathbf{x}}^*) \geq g(\mathbf{x}_1) > g(\mathbf{x}_2) > g(\tilde{\mathbf{x}}^*)$, then $f(\mathbf{x}_1) \geq f(\mathbf{x}_2)$.*

This assumption is similar in nature to Assumption 3, but has a slightly stronger condition on the the local monotonicity region.

Proposition 4 (Bounded cost change in FLOW²). *Under Assumption 4, $g(\mathbf{x}_{k+1}) \leq g(\mathbf{x}_k)C, \forall k$.*

Proposition 5 (Bounded evaluation cost for any function evaluation of FLOW²). *Under Assumption 4 and Assumption 5, $g(\mathbf{x}_k) \leq g(\tilde{\mathbf{x}}^*)C, \forall k$.*

Proposition 4 and 5 are similar to Proposition 2 and 3 respectively, but have a multiplicative form on the cost bound.

Theorem 4 (Expected total evaluation cost of FLOW²). *Under Assumption 4 and Assumption 5, if $K^* \leq \lceil \frac{\log \gamma}{\log C} \rceil$, $T \leq g(\tilde{\mathbf{x}}^*) \cdot \frac{2(\gamma-1)C}{\gamma(C-1)}$; else, $T \leq g(\tilde{\mathbf{x}}^*) \cdot 2C(K^*C + \frac{\gamma-1}{\gamma(C-1)} - \frac{\log \gamma}{\log C}C + C)$, in which $\gamma = \frac{g(\tilde{\mathbf{x}}^*)}{g(\mathbf{x}_0)} > 1$.*

Proof idea The proof of Theorem 4 is similar to that of Theorem 3 and is provided in Appendix B.

Remark 2 (Comparison between Theorem 3 and 4). *In Theorem 4, the factorized form of the cost function ensures that the cost bound sequence begins as a geometric series until it gets close to the optimal configuration’s cost, such that the summation of this subsequence remains a constant factor times the optimal configuration’s cost. It suggests that the expected total cost for obtaining a ϵ -approximation of the loss is $O(1)$ times that minimal cost compared to $O(de^{-2})$ when $K^* \leq \min\{\lceil \frac{\log(g(\bar{\mathbf{x}}^*)/g(\mathbf{x}_0))}{\log C} \rceil, \lceil \frac{(g(\bar{\mathbf{x}}^*)-g(\mathbf{x}_0))}{D} \rceil\}$.*

Remark 3 (Implication of Theorem 3 and 4). *By comparing Theorem 4 to Theorem 3, we can see that the factorized form does not affect the asymptotic form of the overall cost bound. It improves a constant term in the overall cost bound, and should be used if the relation of the cost function with respect to hyperparameter is known. But even when such information is unknown and the factorized form is not available, the asymptotic cost bound in Theorem 4 still applies.*

Our analysis above shows that a factorized form of cost function stated in Assumption 4 brings extra benefits in controlling the expected total cost. Here we illustrate how can we use proper transformation functions to map the original problem space to a space where the factorized form in Assumption 4 is satisfied in case such assumption is not satisfied in terms of the original hyperparameter variable.

Remark 4 (Use transformation functions to realize Assumption 4). *Here we introduce a new set of notations corresponding to the original hyperparameter variables that need to be transformed. Denote $\mathbf{h} \in \mathcal{H}$ as the original hyperparameter variable in the hyperparameter space \mathcal{H} . Denote $l(\mathbf{h})$ as the validation loss using hyperparameter \mathbf{h} and denote $t(\mathbf{h})$ as the evaluation cost using \mathbf{h} . Mapping back to our previous notations, $f(\mathbf{x}) = l(\mathbf{h})$, and $t(\mathbf{h}) = g(\mathbf{x})$. Let’s assume the dominant part of the cost t can be written into: $t(\mathbf{h}) = \prod_{i=1}^{d'} S_i(\mathbf{h})$, where $d' \leq d$ and $S_i(\cdot) : \mathbb{R}^d \rightarrow \mathbb{R}^+$, and $S(\mathbf{h}) = (S_1(\mathbf{h}), S_2(\mathbf{h}), \dots, S_d(\mathbf{h})) : \mathbb{R}^d \rightarrow \mathbb{R}^{+d}$ has a reverse mapping \tilde{S} , i.e., $\forall \mathbf{h} \in \mathcal{H}, \tilde{S}(S(\mathbf{h})) = \mathbf{h}$.*

Such transformation function pairs can be easily constructed if the computational complexity of the ML algorithm with respect to the hyperparameters is known. For example, if $\mathbf{h} = (h_1, h_2, \dots, h_5)$, and the complexity of the training algorithm is $t(\mathbf{h}) = \Theta(h_1^2 h_2^{-1/2} 2^{h_3} \log h_4)$, where h_1 and h_2 are positive numbers, and $h_4 > 1$, we can let $S_1(\mathbf{h}) = h_1^2, S_2(\mathbf{h}) = h_2^{-1/2}, S_3(\mathbf{h}) = 2^{h_3}, S_4(\mathbf{h}) = \log h_4, S_5(\mathbf{h}) = h_5, d' = 4$. With the transformation function pair S and \tilde{S} introduced, we define $\mathbf{x} := \log S(\mathbf{h})$. Then we have $\mathbf{h} = \tilde{S}(e^{\mathbf{x}})$, $f(\mathbf{x}) = l(\mathbf{h}) = l(\tilde{S}(e^{\mathbf{x}}))$ and $g(\mathbf{x}) = t(\mathbf{h}) = t(\tilde{S}(e^{\mathbf{x}})) = \prod_{i=1}^d e^{x_i}$, which realize Assumption 4.

Let us use hyperparameter tuning for XGBoost as a more concrete example in the HPO context. In XGBoost, cost-related hyperparameter include $h_1 = \text{tree num}, h_2 =$

$\text{leaf num}, h_3 = \text{min child weight}$. The correlation between evaluation cost and hyperparameter is $t(\mathbf{h}) = \Theta(h_1 \times h_2/h_3)$. Using a commonly used log transformation, $x_i = \log h_i$ for $i \in [d]$ (i.e., $S_i(\mathbf{h}) = h_i$ for $i \in [d]$), we have $g(\mathbf{x}) = \Theta(e^{x_1} \times e^{x_2} \times e^{-x_3})$, which again satisfies Assumption 4.

3.5. Cost effective HPO using FLOW²

We showed that the proposed randomized direct search method FLOW² can achieve both small numbers of iterations before convergence and bounded cost each per iteration. But FLOW² itself is not readily applicable for HPO problems because (1) the possibility of getting stuck into local optima; (2) the setting of stepsize (the convergence condition of FLOW² requires it to be related with the total number of iterations, which may not be available in a HPO problem); and (3) the existence of discrete hyperparameters. In order to address these limitations and make our solution an off-the-shelf HPO solution, we equip FLOW² with random restart, adaptive stepsize and optimization variable projection. Here we provide a brief description of the major components in the final HPO solution CEO and present the details of it in Algorithm 2 in Appendix C.1.

CEO needs the following information as input: (I1) the feasible configuration search space \mathcal{X} . (I2) a low-cost initial configuration \mathbf{x}_0 : CEO requires the input starting point \mathbf{x}_0 in FLOW² to be a low-cost point, according to the cost analysis in Section 3.4. Any configuration whose cost is smaller than the optimal configuration’s cost can be considered as a low-cost initial configuration, for example it can be set as $\arg \min_{\mathbf{x}} g(\mathbf{x})$. (I3) (optionally) the transformation function $S(\cdot)$ and its reverse $\tilde{S}(\cdot)$: they can be constructed following the instructions in Remark 4 if the relation between hyperparameter and cost is known. Otherwise, identity functions can be used without validation of the cost bound.

After initialization, at each iteration k , CEO calls FLOW² to select new points, i.e., $\mathbf{x}_k \pm \mathbf{u}_k$, to evaluate and report the model trained with the corresponding configurations. After executing one iteration of FLOW², CEO dynamically adjusts the stepsize δ_k and periodically resets FLOW² when necessary. In the following discussion, we describe how CEO handles discrete variables using projection, dynamically adjusts stepsize, and performs the periodic reset.

Projection of the optimization variable during function evaluation. In practice, the newly proposed configuration $\mathbf{x}_k \pm \mathbf{u}_k$ is not necessarily in the feasible hyperparameter space, especially when discrete hyperparameter exists. In such scenarios, we use a projection function $\text{Proj}_{\mathcal{X}}(\cdot)$ to map the proposed new configuration to the feasible space (More Details are provided in Appendix C.1).

Dynamic adjustments of stepsize δ_k . According to the convergence analysis in Section 3.3, to achieve the proved convergence rate, δ_k , i.e., the stepsize of FLOW² at iteration k , needs to be set as $O(\frac{1}{\sqrt{K}})$, in which K is the total number of iterations. However in practical HPO scenarios, K is usually unknown beforehand. CEO starts from a relative large setting of stepsize (i.e., assuming a small K) and gradually adjust it depending our estimation of K . Specifically, we record the number n of consecutively no improvement iterations, and decrease stepsize once n is larger than a threshold N . Let K_{old} denote the number of iterations till the last decrease of δ_k (or the iterations taken to find a best configuration in the current round before any decrease), and K_{new} denote the total iteration number in the current round. According to the convergence analysis, δ_k should be changed from $O(\sqrt{\frac{1}{K_{\text{old}}}})$ to $O(\sqrt{\frac{1}{K_{\text{new}}}})$. Based on this insight, we set $\delta_{k+1} = \delta_k \sqrt{\frac{K_{\text{old}}}{K_{\text{new}}}}$. In order to prevent δ_k from becoming too small, we also impose a lower bound on it and stop decreasing δ_k once it reaches the lower bound. (The justification for the setting of N and the lower bound on the δ_k is provided in Appendix C.1).

Periodic reset of FLOW² and randomized initialization. The loss functions in HPO problems are usually non-convex. In such non-convex problems, the first-order stationary point can be a saddle point or local minimum. Because of the randomized search in FLOW², it is very likely that FLOW² can escape from saddle points easily (Jin et al., 2017). To increase the chance of escaping from local optimum too, once the stepsize δ_k is decreased to a very small value, i.e., its lower bound δ_{lower} , we restart the search from a random point and increase the largest stepsize in the new search round. The random point can be generated in various ways; for example, it can be generated by adding a Gaussian noise g to the original initial point \mathbf{x}_0 .

4. Experiment

We perform an extensive experimental study using a latest open source AutoML benchmark (Gijsbers et al., 2019), which includes 39 classification tasks. Each task consists of a dataset in 10 folds, and a metric to optimize. Since this benchmark does not include regression tasks, we enriched it with 14 regression tasks² from a machine learning evaluation benchmark PMLB (Olson et al., 2017). All the datasets are available on OpenML. The number of instances in these datasets ranges from 748 to 1 million, and the number of features ranges from 4 to 7200. Roc-auc is used as the optimization metric for binary tasks, log-loss for multi-class tasks, and r2 score for regression tasks.

² Among the 120 OpenML regression datasets in PMLB, we selected the ones whose numbers of instances are larger than 10,000.

4.1. Baselines and evaluation setup

We include 5 representative HPO methods as baselines including Random search (RS) (Bergstra & Bengio, 2012), Bayesian optimization with Gaussian Process and expected improvement (GPEI) and expected improvement per second (GPEIPerSec) as acquisition function respectively (Snoek et al., 2012), SMAC (Hutter et al., 2011), and BOHB (Falkner et al., 2018). The latter three are all based on Bayesian optimization, and BOHB was shown to be the state of the art multi-fidelity method (e.g., outperforming Hyperband and FABOLAS). In addition to these existing HPO methods, we also include an additional method CEO-0, which uses the same framework as CEO but replaces FLOW² with the zeroth-order optimization method ZOGD (Nesterov & Spokoiny, 2017). Notice that like FLOW², ZOGD is not readily applicable to the HPO problem. While the CEO framework permits ZOGD to be used as an alternative local search method, the comparison between CEO-0 and CEO would allow us to evaluate the contribution of FLOW² in controlling the cost in CEO.

We compare their performance in tuning 9 hyperparameters for XGBoost. XGBoost is good for testing because it is one of the most commonly used libraries in many machine learning competitions and applications. Evaluating all the 7 methods on 47 tasks³ in the enriched AutoML benchmark using one CPU hour budget for each of the 10 folds in each task takes $7 \times 47 \times 10 = 3290$ CPU hours, or 4.5 CPU months. Additional details can be found in Appendix C.2. In addition to XGBoost, we also evaluated all the methods on deep neural networks. Since the experiment setup and comparison conclusion are similar to those in the XGBoost experiment, we include the detailed experiment setup and results on deep neural networks in Appendix C.2.

4.2. Performance comparison

Performance curve To investigate the effectiveness of CEO’s cost control, we visualize the performance curve in term of validation loss of all the methods over an one-hour wall clock time period. Due to space limit, we include the performance curves on 6 datasets in Figure 1 and put the rest in the appendix. These 6 datasets represent a diverse group: The two rows in Figure 1 include three small datasets and large datasets respectively. In each row, the three datasets are for binary classification, multi-class classification, and regression task respectively.

The curves show that overall it takes RS and classical BO-based methods much longer time to reach low loss, because they are prone to trying unnecessarily expensive configurations. Although GPEIPerSec considers cost when deciding

³We exclude the largest 6 tasks because they require much longer time to converge for all the methods.

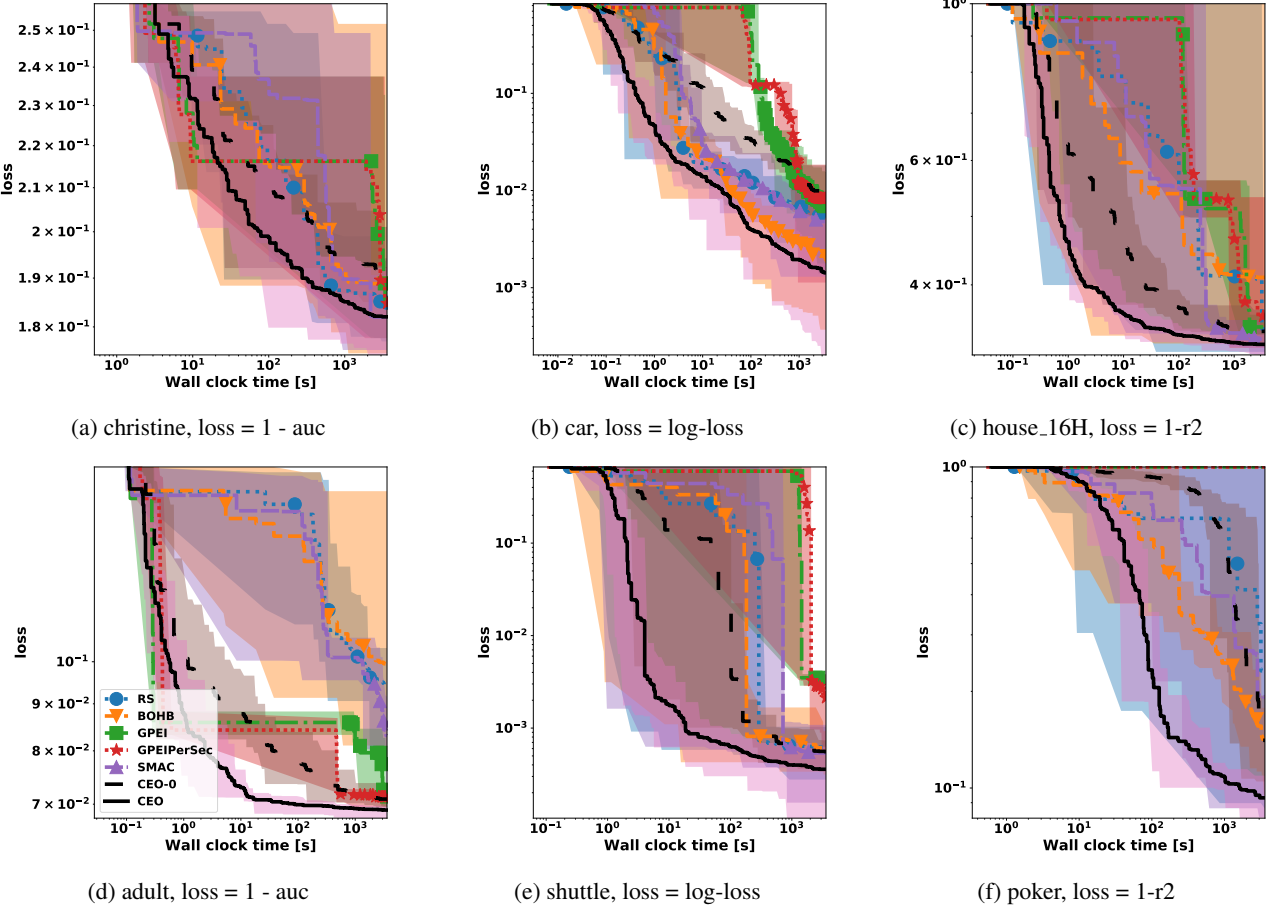


Figure 1. Optimization performance curve. Lines correspond to mean loss over 10 folds, and shades correspond to max and min loss

which hyperparameters to try, it depends on a probabilistic model that needs many evaluation results (already costly) to make a good estimation of the cost. In addition, when the time budget is sufficiently large, it may suffer because of its penalization on good but expensive configurations. In our experiments, GPEIPerSec outperforms GPEI in some cases (for example, *adult*) but tends to underperform GPEI on small datasets (for example, *car*). Since *CEO* is able to effectively control the evaluation cost invoked during the optimization process, overall its performance is the best on all the datasets. *CEO-0* can leverage the correlation in the same way. However due to the unique designs in *FLOW*², *CEO* still maintains its leading performance. In summary, *CEO* demonstrates strong anytime performance. It achieves up to three orders of magnitude speedup comparing to other methods for reaching any loss level.

Overall optimality of loss and cost Table 1 shows the final loss and the cost used to reach that loss per method per dataset. Here optimality is considered as the best performance that can be reached within the one-hour time budget by all the compared methods. Meanings of the numbers in

Table 1 are explained in the table caption. On the one hand, we can compare all the methods' capability of finding best loss within the given time budget. On the other hand, for those methods which can find the best loss within the time budget, we can compare the time cost taken to find it.

Specifically, we can see that *CEO* is able to find the best loss on almost all the datasets. For example, on *Airlines*, *CEO* can find a configuration with a scaled score (high score corresponds to low loss) of 1.3996 in 3285 seconds, while existing RS and BO methods report more than 16% lower score in the one-hour time budget and *CEO-0* is 5.6% lower. For the cases where the optimality can be reached by both *CEO* and at least one baseline, *CEO* almost always takes the least amount of cost. For example, on *shuttle*, all the methods except GPEI and GPEIPerSec can reach a scaled score of 0.9999. It only takes *CEO* 72 seconds. Other methods show 6× to 26× slowdowns for reaching it. Overall Table 1 shows that *CEO* has a dominating advantage over all the others in reaching the same or better loss within the least amount of time.

Table 1. Optimality of score and cost for XGBoost. We scale the original scores for classification tasks following the referred AutoML benchmark: 0 corresponds to a constant class prior predictor, and 1 corresponds to a tuned random forest. Bold numbers are best scaled score and lowest cost to find it among all the methods within given budget. For methods which cannot find best score after given budget, we show the score difference compared to the best score, e.g., -1% means 1 percent lower score than best. For methods which can find best score with suboptimal cost, we show the cost difference compared to the best cost, e.g., $\times 10$ means 10 times higher cost than best

Dataset (* for regression)	RS	BOHB	GPEI	GPEIPerSec	SMAC	CEO-0	CEO
adult	-5.9%	-7.1%	-0.6%	-0.5%	-3.3%	-0.4%	1.0524 (1199s)
Airlines	-37.3%	-33.3%	-16.2%	-16.2%	-37.2%	-5.6%	1.3996 (3285s)
Amazon_employee_acce	-8.9%	-0.3%	-5.5%	-6.7%	-0.9%	-3.9%	1.0008 (3499s)
APSFailure	-0.1%	-0.1%	-0.5%	-0.5%	-0.2%	-0.2%	1.0050 (1913s)
Australian	-0.7%	-0.8%	-2.2%	-2.1%	-0.5%	-0.6%	1.0695 (3041s)
bank_marketing	-2.4%	$\times 2.8$	-1.4%	-0.7%	-0.4%	-0.4%	1.0091 (1265s)
blood_transfusion	-26.2%	-3.0%	-11.1%	-10.6%	-2.5%	-1.7%	1.6565 (3200s)
car	-0.5%	-0.1%	-0.7%	-0.8%	-0.4%	-1.0%	1.0578 (1337s)
christine	-0.9%	-2.1%	-0.9%	-0.9%	$\times 1.2$	-2.8%	1.0281 (3108s)
cnae_9	-9.9%	1.0803 (2744s)	-0.5%	-0.9%	-0.3%	-2.2%	-0.4%
connect_4	-12.7%	-5.9%	-5.9%	-6.0%	-1.9%	-3.9%	1.3918 (3136s)
credit_g	-1.3%	-1.7%	-4.0%	-4.8%	-0.1%	-1.4%	1.1924 (3477s)
fabert	-2.2%	-1.0%	-17.5%	-36.2%	-1.9%	-7.4%	1.0805 (3487s)
Helena	-51.6%	-54.0%	-82.3%	-82.3%	-56.4%	-31.7%	5.2707 (3469s)
higgs	-5.0%	-0.5%	-5.4%	-3.1%	-0.7%	-2.0%	1.0180 (1962s)
Jannis	-36.1%	-48.8%	-73.0%	-55.5%	-6.8%	-10.8%	1.2316 (3482s)
jasmine	-0.9%	-0.3%	-1.6%	-0.8%	-0.6%	-2.4%	1.0083 (3319s)
jungle_chess_2pcs_ra	-4.6%	-3.8%	-3.0%	-2.6%	-2.5%	-1.0%	1.3209 (3094s)
kc1	-1.5%	0.9406 (2324s)	-4.0%	-5.9%	-1.5%	-2.5%	-0.4%
KDDCup09_appetency	-6.4%	-2.6%	-7.0%	-6.5%	-0.7%	-1.1%	1.1778 (2140s)
kr-vs-kp	-1.1%	$\times 1.4$	$\times 309.6$	$\times 714.2$	$\times 1.4$	$\times 70.2$	1.0002 (5s)
mfeat_factors	-0.3%	-6.4%	-0.9%	-0.6%	-0.3%	-0.6%	1.0676 (1845s)
MiniBooNE	-1.4%	-0.1%	-4.2%	-2.3%	$\times 2.8$	-1.1%	1.0100 (887s)
nomao	$\times 1.3$	$\times 1.5$	$\times 1.9$	-0.1%	$\times 1.3$	-0.2%	1.0022 (728s)
numeraid28.6	-13.8%	-12.6%	-11.4%	-10.5%	-6.9%	-2.2%	1.5941 (3559s)
phoneme	-2.7%	-0.1%	-0.1%	-0.3%	-0.2%	-0.4%	0.9938 (2341s)
segment	-0.3%	-6.2%	-0.6%	-0.8%	-0.2%	-0.5%	1.0084 (3284s)
shuttle	$\times 6.4$	$\times 26.3$	-0.5%	-0.3%	$\times 10.7$	$\times 10.4$	0.9999 (72s)
sylvine	-0.1%	1.0071 (1680s)	-0.1%	-0.3%	-0.1%	-0.4%	$\times 2.1$
vehicle	-1.9%	-0.9%	-4.3%	-5.5%	-1.7%	-2.1%	1.0892 (2685s)
volkert	-30.8%	-30.7%	-91.1%	-91.1%	-43.4%	-13.7%	1.2152 (3244s)
2dplanes*	-4.9%	-3.8%	-0.2%	-0.1%	-2.5%	$\times 5.1$	0.9479 (7s)
bng_breastTumor*	-32.8%	-4.9%	-3.0%	-6.8%	-13.1%	-1.3%	0.1772 (2994s)
bng_ecomonths*	-0.9%	-0.2%	-0.9%	-4.5%	-0.6%	-0.9%	0.4739 (2563s)
bng_lowbwt*	-0.4%	-10.8%	-0.2%	-1.3%	-10.2%	-1.8%	0.6175 (466s)
bng_pbc*	-32.0%	-20.7%	-10.5%	-4.9%	-23.5%	-2.5%	0.4514 (3266s)
bng_pharynx*	-20.7%	-12.2%	-1.2%	-1.0%	-1.8%	-0.2%	0.5140 (2760s)
bng_pwLinear*	-14.3%	-6.3%	-0.7%	-0.7%	-0.7%	$\times 9.9$	0.6222 (316s)
fried*	-0.1%	-10.0%	-0.1%	-0.4%	-0.1%	-0.4%	0.9569 (654s)
houses*	-0.6%	-10.5%	-1.4%	-1.9%	-0.1%	-1.1%	0.8526 (1979s)
house_8L*	-11.1%	-1.1%	-5.5%	-4.7%	-0.9%	-0.6%	0.6913 (2675s)
house_16H*	-2.0%	-12.0%	-2.9%	-4.7%	-0.8%	-2.1%	0.6702 (2462s)
mv*	-8.7%	$\times 27.4$	$\times 13.8$	$\times 92.2$	$\times 25.4$	$\times 6.7$	0.9995 (10s)
poker*	-15.3%	-5.4%	-100.0%	-100.0%	-10.9%	-5.2%	0.9068 (3407s)
pol*	-0.1%	$\times 3.2$	-0.2%	-0.3%	$\times 3.7$	-0.1%	0.9897 (712s)

5. Conclusion and Future Work

This work addresses the efficiency of HPO from the cost perspective. We propose a new randomized direct search method FLOW^2 specifically designed for cost-effective derivative-free optimization. FLOW^2 has a provable convergence rate and cost bound. The cost bound illustrates how much our cost can be comparing to the optimal configurations cost depending on different initial points. Such a cost bound does not exist in any HPO literature. We also present an improved cost bound by leveraging the computational complexity of a machine learning algorithm with respect to its hyperparameters if such complexity is known. Equipping FLOW^2 with random restart, step sizes following its convergence analysis, and other practical adjustments, we obtain a cost-effective HPO method CEO with strong anytime performance and final performance.

As future work, it is worth studying whether we can further improve CEO by incorporating Bayesian optimization into it. For example, Bayesian optimization can be used to decide the starting point of each round of FLOW^2 's search when it is restarted. In addition, CEO only considers the HPO scenario where all hyperparameters are numerical. It is also worth studying how to incorporate categorical hyperparameters into the framework of CEO . For example, one straightforward way to incorporate categorical hyperparameter is to randomly generate a configuration of the categorical hyperparameters whenever FLOW^2 restarted.

References

Bergstra, J. and Bengio, Y. Random search for hyperparameter optimization. *J. Mach. Learn. Res.*, 13:281–305, February 2012.

Bergstra, J. S., Bardenet, R., Bengio, Y., and Kégl, B. Algorithms for hyper-parameter optimization. In *Advances in neural information processing systems*, pp. 2546–2554, 2011.

Brochu, E., Cora, V. M., and de Freitas, N. A tutorial on bayesian optimization of expensive cost functions, with application to active user modeling and hierarchical reinforcement learning. *CoRR*, abs/1012.2599, 2010.

Bull, A. D. Convergence rates of efficient global optimization algorithms. *J. Mach. Learn. Res.*, 12:28792904, November 2011.

Chen, T. and Guestrin, C. Xgboost: A scalable tree boosting system. In *KDD*, 2016.

Falkner, S., Klein, A., and Hutter, F. BOHB: Robust and efficient hyperparameter optimization at scale. In *Proceedings of the 35th International Conference on Machine Learning (ICML 2018)*, 2018.

Gijsbers, P., LeDell, E., Thomas, J., Poirier, S., Bischi, B., and Vanschoren, J. An open source automl benchmark. In *AutoML Workshop at ICML 2019*, 2019.

Hutter, F., Hoos, H. H., and Leyton-Brown, K. Sequential model-based optimization for general algorithm configuration. In *Learning and Intelligent Optimization*, 2011.

Jin, C., Ge, R., Netrapalli, P., Kakade, S. M., and Jordan, M. I. How to escape saddle points efficiently. In *Proceedings of the 34th International Conference on Machine Learning*, pp. 1724–1732, 2017.

Kandasamy, K., Dasarathy, G., Schneider, J., and Póczos, B. Multi-fidelity bayesian optimisation with continuous approximations. In *Proceedings of the 34th International Conference on Machine Learning*, pp. 1799–1808, 2017.

Klein, A., Falkner, S., Bartels, S., Hennig, P., and Hutter, F. Fast bayesian optimization of machine learning hyperparameters on large datasets. In *Artificial Intelligence and Statistics*, pp. 528–536, 2017.

Kolda, T. G., Lewis, R. M., and Torczon, V. Optimization by direct search: New perspectives on some classical and modern methods. *SIAM Review*, 45(3):385–482, 2003.

Li, L., Jamieson, K., DeSalvo, G., Rostamizadeh, A., and Talwalkar, A. Hyperband: A novel bandit-based approach to hyperparameter optimization. In *ICLR'17*, 2017.

Liu, S., Chen, P. Y., Chen, X., and Hong, M. Signsgrd via zeroth-order oracle. In *7th International Conference on Learning Representations, ICLR 2019*, 2019.

Lu, Z., Chen, L., Chiang, C.-K., and Sha, F. Hyperparameter tuning under a budget constraint. In *Proceedings of the Twenty-Eighth International Joint Conference on Artificial Intelligence, IJCAI-19*, pp. 5744–5750, 2019.

Nesterov, Y. and Spokoiny, V. Random gradient-free minimization of convex functions. *Foundations of Computational Mathematics*, 17(2):527–566, 2017.

Olson, R. S., La Cava, W., Orzechowski, P., Urbanowicz, R. J., and Moore, J. H. Pmlb: a large benchmark suite for machine learning evaluation and comparison. *BioData Mining*, 10(1):36, Dec 2017.

Snoek, J., Larochelle, H., and Adams, R. P. Practical bayesian optimization of machine learning algorithms. In *Advances in neural information processing systems*, pp. 2951–2959, 2012.

A. Proofs about Convergence Analysis

A.1. Facts and definitions

Fact 2 (Directional derivative). *Here we list several facts about the directional derivative $f'_u(\mathbf{x})$ that will be used in our following proof.*

Definition of $f'_u(\mathbf{x})$: $f'_u(\mathbf{x}) = \lim_{\delta \rightarrow 0} \frac{f(\mathbf{x} + \delta \mathbf{u}) - f(\mathbf{x})}{\delta}$

Properties: $f'_u(\mathbf{x}) = \nabla f(\mathbf{x})^\top \mathbf{u}$, $f'_{-\mathbf{u}}(\mathbf{x}) = -f'_u(\mathbf{x})$

We define,

$$\begin{aligned}\tilde{\mathbb{S}}_{\mathbf{x}}^- &:= \{\mathbf{u} \in \mathbb{S} \mid f'_u(\mathbf{x}) \leq -\frac{L\delta}{2}\}, \quad \tilde{\mathbb{S}}_{\mathbf{x}}^+ := \{\mathbf{u} \in \mathbb{S} \mid f'_u(\mathbf{x}) \geq \frac{L\delta}{2}\}, \quad \tilde{\mathbb{S}}_{\mathbf{x}}^\# := \{\mathbf{u} \in \mathbb{S} \mid |f'_u(\mathbf{x})| \leq \frac{L\delta}{2}\} \\ \mathbb{S}_{\mathbf{x}}^- &:= \{\mathbf{u} \in \mathbb{S} \mid f(\mathbf{x} + \delta \mathbf{u}) - f(\mathbf{x}) < 0\}, \quad \mathbb{S}_{\mathbf{x}}^{+-} := \{\mathbf{u} \in \mathbb{S} \mid f(\mathbf{x} + \delta \mathbf{u}) - f(\mathbf{x}) > 0, f(\mathbf{x} - \delta \mathbf{u}) - f(\mathbf{x}) < 0\}\end{aligned}$$

A.2. Technical lemmas

Lemma 1. $\tilde{\mathbb{S}}_{\mathbf{x}}^+$ and $\tilde{\mathbb{S}}_{\mathbf{x}}^-$ are symmetric, i.e. $\tilde{\mathbb{S}}_{\mathbf{x}}^+ = \{-\mathbf{u} \mid \mathbf{u} \in \tilde{\mathbb{S}}_{\mathbf{x}}^-\}$ and $\tilde{\mathbb{S}}_{\mathbf{x}}^- = \{-\mathbf{u} \mid \mathbf{u} \in \tilde{\mathbb{S}}_{\mathbf{x}}^+\}$.

Proof of Lemma 1. According to the definition of directional derivative, we have $f'_{-\mathbf{u}}(\mathbf{x}) = -f'_u(\mathbf{x})$. Then $\forall \mathbf{u} \in \tilde{\mathbb{S}}_{\mathbf{x}}^+$, suppose $f'_u(\mathbf{x}) = a_u < \frac{L\delta}{2}$, then we have $f'_{-\mathbf{u}}(\mathbf{x}) = -f'_u(\mathbf{x}) = -a_u < -\frac{L\delta}{2}$, i.e. $-\mathbf{u} \in \tilde{\mathbb{S}}_{\mathbf{x}}^+$. Similarly, we can prove when $\forall \mathbf{u} \in \tilde{\mathbb{S}}_{\mathbf{x}}^+$, $-\mathbf{u} \in \tilde{\mathbb{S}}_{\mathbf{x}}^-$.

Intuitively it means that if we walk (in the domain) in one direction to make $f(\mathbf{x})$ go up, then walking in the opposite direction should make it go down. \square

Lemma 2. Under Assumption 1, we have,

$$(1) |f'_u(\mathbf{x})| > \frac{L\delta}{2} \Rightarrow \text{sign}(f(\mathbf{x} + \delta \mathbf{u}) - f(\mathbf{x})) = \text{sign}(f'_u(\mathbf{x})).$$

$$(2) \tilde{\mathbb{S}}_{\mathbf{x}}^- \subseteq \mathbb{S}_{\mathbf{x}}^-. \quad (3) \tilde{\mathbb{S}}_{\mathbf{x}}^+ \subseteq \mathbb{S}_{\mathbf{x}}^{+-}.$$

Proof of Lemma 2. Proof of (1): According to the smoothness assumption specified in Assumption 1:

$$|f(\mathbf{y}) - f(\mathbf{x}) - \nabla f(\mathbf{x})^\top (\mathbf{y} - \mathbf{x})| \leq \frac{L}{2} \|\mathbf{y} - \mathbf{x}\|^2$$

By letting $\mathbf{y} = \mathbf{x} + \delta \mathbf{u}$, we have $|f(\mathbf{x} + \delta \mathbf{u}) - f(\mathbf{x}) - \delta \nabla f(\mathbf{x})^\top \mathbf{u}| \leq \frac{L\delta^2}{2}$, which is $\left| \frac{f(\mathbf{x} + \delta \mathbf{u}) - f(\mathbf{x})}{\delta} - f'_u(\mathbf{x}) \right| \leq \frac{L\delta}{2}$, i.e.,

$$f'_u(\mathbf{x}) - \frac{L\delta}{2} \leq \frac{f(\mathbf{x} + \delta \mathbf{u}) - f(\mathbf{x})}{\delta} \leq f'_u(\mathbf{x}) + \frac{L\delta}{2}$$

So $f'_u(\mathbf{x}) > \frac{L\delta}{2} \Rightarrow \frac{f(\mathbf{x} + \delta \mathbf{u}) - f(\mathbf{x})}{\delta} > 0$, and $f'_u(\mathbf{x}) < -\frac{L\delta}{2} \Rightarrow \frac{f(\mathbf{x} + \delta \mathbf{u}) - f(\mathbf{x})}{\delta} < 0$. Combinning them, we have when $|f'_u(\mathbf{x})| > \frac{L\delta}{2}$, $\text{sign}(f'_u(\mathbf{x})) = \text{sign}(\frac{f(\mathbf{x} + \delta \mathbf{u}) - f(\mathbf{x})}{\delta}) = \text{sign}(f(\mathbf{x} + \delta \mathbf{u}) - f(\mathbf{x}))$, which proves conclusion (1).

Proof of (2): When $\mathbf{u} \in \tilde{\mathbb{S}}_{\mathbf{x}}^-$, $f'_u(\mathbf{x}) < -\frac{L\delta}{2}$, then according to conclusion (1), $\text{sign}(f(\mathbf{x} + \delta \mathbf{u}) - f(\mathbf{x})) = \text{sign}(f'_u(\mathbf{x})) < 0$, i.e. $\mathbf{u} \in \mathbb{S}_{\mathbf{x}}^-$. So we have $\tilde{\mathbb{S}}_{\mathbf{x}}^- \subseteq \mathbb{S}_{\mathbf{x}}^-$.

Proof of (3): Similarly, when $\mathbf{u} \in \tilde{\mathbb{S}}_{\mathbf{x}}^+$, $f'_u(\mathbf{x}) > \frac{L\delta}{2}$, then according to conclusion in (1), we have $\text{sign}(f(\mathbf{x} + \delta \mathbf{u}) - f(\mathbf{x})) = \text{sign}(f'_u(\mathbf{x})) > 0$ and $-\text{sign}(f(\mathbf{x} - \delta \mathbf{u}) - f(\mathbf{x})) = -\text{sign}(f'_{-\mathbf{u}}(\mathbf{x})) = \text{sign}(f'_u(\mathbf{x})) > 0$, which means that $\mathbf{u} \in \mathbb{S}_{\mathbf{x}}^{+-}$. So we have $\tilde{\mathbb{S}}_{\mathbf{x}}^+ \subseteq \mathbb{S}_{\mathbf{x}}^{+-}$. \square

Lemma 3. For any $\mathbf{x} \in \mathcal{X}$,

$$\mathbb{E}_{\mathbf{u} \in \mathbb{S}} [|f'_u(\mathbf{x})|] = \frac{2\Gamma(\frac{d}{2})}{(d-1)\Gamma(\frac{d-1}{2})\sqrt{\pi}} \|\nabla f(\mathbf{x})\|_2 \quad (8)$$

Proof of Lemma 3. According to the definition of directional derivative

$$\begin{aligned}\mathbb{E}_{\mathbf{u} \in \mathbb{S}}[|f'_{\mathbf{u}}(\mathbf{x}_k)|] &= \mathbb{E}_{\mathbf{u} \in \mathbb{S}}[|\nabla f(\mathbf{x}_k)^T \mathbf{u}|] = \|\nabla f(\mathbf{x}_k)\|_2 \mathbb{E}_{\mathbf{u} \in \mathbb{S}}[|\cos(\theta_{\mathbf{u}})|] = \|\nabla f(\mathbf{x}_k)\|_2 \mathbb{E}_{\mathbf{u} \in \mathbb{S}}[|u_1|] \\ &= \frac{2\Gamma(\frac{d}{2})}{(d-1)\Gamma(\frac{d-1}{2})\sqrt{\pi}} \|\nabla f(\mathbf{x}_k)\|_2\end{aligned}\quad (9)$$

where $\theta_{\mathbf{u}}$ is the angle between \mathbf{u} and $\nabla f(\mathbf{x}_k)$, and $\Gamma(\cdot)$ is the gamma function. The last equality can be derived by calculating the expected absolute value of a coordinate $|u_1|$ of a random unit vector⁴. \square

A.3. Full proof of Proposition 1, Theorem 1 and Theorem 2

Proof of Proposition 1. To simplify notations, we denote $\mathbf{z}_{k+1} = \nabla f(\mathbf{x}_k)^T(\mathbf{x}_{k+1} - \mathbf{x}_k) + \frac{L}{2}\|\mathbf{x}_{k+1} - \mathbf{x}_k\|^2$. Denote the volume of a particular surface area as $\text{Vol}(\cdot)$.

According to Assumption 1, we have, $f(\mathbf{x}_{k+1}) - f(\mathbf{x}_k) \leq \mathbf{z}_{k+1}$. By taking expectation on both sides of this inequality, we have,

$$\mathbb{E}_{\mathbf{u}_k \in \mathbb{S}}[f(\mathbf{x}_{k+1}) - f(\mathbf{x}_k)] \leq \frac{\text{Vol}(\tilde{\mathbb{S}}_{\mathbf{x}_k}^-)}{\text{Vol}(\mathbb{S})} \mathbb{E}_{\mathbf{u} \in \tilde{\mathbb{S}}_{\mathbf{x}_k}^-}[\mathbf{z}_{k+1}] + \frac{\text{Vol}(\tilde{\mathbb{S}}_{\mathbf{x}_k}^+)}{\text{Vol}(\mathbb{S})} \mathbb{E}_{\mathbf{u} \in \tilde{\mathbb{S}}_{\mathbf{x}_k}^+}[\mathbf{z}_{k+1}] \quad (10)$$

The update rules in line 5 and line 8 of Alg 1 can be equivalently written into the following equations respectively,

$$\mathbf{x}_{k+1} = \mathbf{x}_k - \delta \text{sign}(f(\mathbf{x}_k + \delta \mathbf{u}_k) - f(\mathbf{x}_k)) \mathbf{u}_k \quad (11)$$

$$\mathbf{x}_{k+1} = \mathbf{x}_k - \delta \text{sign}(f(\mathbf{x}_k - \delta \mathbf{u}_k) - f(\mathbf{x}_k))(-\mathbf{u}_k) \quad (12)$$

According to conclusion (2) in Lemma 2, $\tilde{\mathbb{S}}_{\mathbf{x}_k}^- \subseteq \mathbb{S}_{\mathbf{x}_k}^-$. So when $\mathbf{u}_k \in \tilde{\mathbb{S}}_{\mathbf{x}_k}^-$, line 5 of Alg 1 will be triggered, and we have,

$$\begin{aligned}\mathbb{E}_{\mathbf{u} \in \tilde{\mathbb{S}}_{\mathbf{x}_k}^-}[\mathbf{z}_{k+1}] &= \mathbb{E}_{\mathbf{u} \in \tilde{\mathbb{S}}_{\mathbf{x}_k}^-}[-\delta \text{sign}(f(\mathbf{x}_k + \delta \mathbf{u}) - f(\mathbf{x}_k)) \nabla f(\mathbf{x}_k)^T \mathbf{u}] + \frac{L\delta^2}{2} \\ &= \mathbb{E}_{\mathbf{u} \in \tilde{\mathbb{S}}_{\mathbf{x}_k}^-}[-\delta \text{sign}(f(\mathbf{x}_k + \delta \mathbf{u}) - f(\mathbf{x}_k)) f'_{\mathbf{u}}(\mathbf{x}_k)] + \frac{L\delta^2}{2} \\ &= \mathbb{E}_{\mathbf{u} \in \tilde{\mathbb{S}}_{\mathbf{x}_k}^-}[-\delta \text{sign}(f'_{\mathbf{u}}(\mathbf{x}_k)) f'_{\mathbf{u}}(\mathbf{x}_k)] + \frac{L\delta^2}{2} \\ &= -\delta \mathbb{E}_{\mathbf{u} \in \tilde{\mathbb{S}}_{\mathbf{x}_k}^-}[|f'_{\mathbf{u}}(\mathbf{x}_k)|] + \frac{L\delta^2}{2}\end{aligned}\quad (13)$$

According to conclusion (3) in Lemma 2, $\tilde{\mathbb{S}}_{\mathbf{x}_k}^+ \subseteq \mathbb{S}_{\mathbf{x}_k}^{+-}$, so when $\mathbf{u} \in \tilde{\mathbb{S}}_{\mathbf{x}_k}^+$, line 8 of Alg 1 will be triggered, and we have,

$$\begin{aligned}\mathbb{E}_{\mathbf{u} \in \tilde{\mathbb{S}}_{\mathbf{x}_k}^+}[\mathbf{z}_{k+1}] &= \mathbb{E}_{\mathbf{u} \in \tilde{\mathbb{S}}_{\mathbf{x}_k}^+}[\delta \text{sign}(f(\mathbf{x}_k - \delta \mathbf{u}) - f(\mathbf{x}_k)) \nabla f(\mathbf{x}_k)^T \mathbf{u}] + \frac{L\delta^2}{2} \\ &= \mathbb{E}_{\mathbf{u} \in \tilde{\mathbb{S}}_{\mathbf{x}_k}^+}[-\delta \text{sign}(f(\mathbf{x}_k - \delta \mathbf{u}) - f(\mathbf{x}_k)) f'_{-\mathbf{u}}(\mathbf{x})] + \frac{L\delta^2}{2} \\ &= \mathbb{E}_{\mathbf{u} \in \tilde{\mathbb{S}}_{\mathbf{x}_k}^+}[-\delta \text{sign}(f'_{-\mathbf{u}}(\mathbf{x})) f'_{-\mathbf{u}}(\mathbf{x})] + \frac{L\delta^2}{2} \\ &= -\delta \mathbb{E}_{\mathbf{u} \in \tilde{\mathbb{S}}_{\mathbf{x}_k}^+}[|f'_{-\mathbf{u}}(\mathbf{x})|] + \frac{L\delta^2}{2}\end{aligned}\quad (14)$$

in which the last equality used the fact that $\tilde{\mathbb{S}}_{\mathbf{x}_k}^+$ and $\tilde{\mathbb{S}}_{\mathbf{x}_k}^-$ are symmetric according to Lemma 1.

By substituting Eq (13) and (14) into Eq (10), we have,

$$\mathbb{E}_{\mathbf{u}_k \in \mathbb{S}}[f(\mathbf{x}_{k+1}) - f(\mathbf{x}_k)] \leq 2 \frac{\text{Vol}(\tilde{\mathbb{S}}_{\mathbf{x}_k}^-)}{\text{Vol}(\mathbb{S})} (-\delta \mathbb{E}_{\mathbf{u} \in \tilde{\mathbb{S}}_{\mathbf{x}_k}^-}[|f'_{\mathbf{u}}(\mathbf{x})|] + \frac{L\delta^2}{2}) \quad (15)$$

⁴[stackexchange305888]: S. E. Average absolute value of a coordinate of a random unit vector? Cross Validated. <https://stats.stackexchange.com/q/305888> (version:2018-09-06).

Based on the symmetric property of $\tilde{\mathbb{S}}_{\mathbf{x}_k}^+$ and $\tilde{\mathbb{S}}_{\mathbf{x}_k}^-$, we have,

$$\begin{aligned} \mathbb{E}_{\mathbf{u}_k \in \mathbb{S}} [|f'_{\mathbf{u}_k}(\mathbf{x}_k)|] &= 2 \frac{\text{Vol}(\tilde{\mathbb{S}}_{\mathbf{x}_k}^-)}{\text{Vol}(\mathbb{S})} \mathbb{E}_{\mathbf{u} \in \tilde{\mathbb{S}}_{\mathbf{x}_k}^-} [|f'_{\mathbf{u}}(\mathbf{x}_k)|] + \frac{\text{Vol}(\tilde{\mathbb{S}}_{\mathbf{x}_k}^\#)}{\text{Vol}(\mathbb{S})} \mathbb{E}_{\mathbf{u} \in \tilde{\mathbb{S}}_{\mathbf{x}_k}^\#} [|f'_{\mathbf{u}}(\mathbf{x}_k)|] \\ &\leq 2 \frac{\text{Vol}(\tilde{\mathbb{S}}_{\mathbf{x}_k}^-)}{\text{Vol}(\mathbb{S})} \mathbb{E}_{\mathbf{u} \in \tilde{\mathbb{S}}_{\mathbf{x}_k}^-} [|f'_{\mathbf{u}}(\mathbf{x}_k)|] + (1 - 2 \frac{\text{Vol}(\tilde{\mathbb{S}}_{\mathbf{x}_k}^-)}{\text{Vol}(\mathbb{S})}) \frac{L\delta}{2} \\ &= 2 \frac{\text{Vol}(\tilde{\mathbb{S}}_{\mathbf{x}_k}^-)}{\text{Vol}(\mathbb{S})} (\mathbb{E}_{\mathbf{u} \in \tilde{\mathbb{S}}_{\mathbf{x}_k}^-} [|f'_{\mathbf{u}}(\mathbf{x}_k)|] - \frac{L\delta}{2}) + \frac{L\delta}{2} \end{aligned} \quad (16)$$

Combining Eq (15) and Eq (16), we have,

$$\mathbb{E}_{\mathbf{u}_k \in \mathbb{S}} [f(\mathbf{x}_{k+1}) | \mathbf{x}_k] - f(\mathbf{x}_k) \leq -\delta \mathbb{E}_{\mathbf{u}_k \in \mathbb{S}} [|f'_{\mathbf{u}_k}(\mathbf{x}_k)|] + \frac{L\delta^2}{2} = -\delta c_d \|\nabla f(\mathbf{x}_k)\|_2 + \frac{1}{2} L\delta^2 \quad (17)$$

in which the last inequality is based on Lemma 3. \square

Proof of Theorem 1. Denote by $\mathcal{U}_k = (\mathbf{u}_0, \mathbf{u}_1, \dots, \mathbf{u}_k)$ a random vector composed by independent and identically distributed (i.i.d.) variables $\{\mathbf{u}_k\}_{k \geq 0}$ attached to each iteration of the scheme up to iteration k . Let $\phi_0 = f(\mathbf{x}_0)$ and $\phi_k := \mathbb{E}_{\mathcal{U}_{k-1}} [f(\mathbf{x}_k)]$, $k \geq 1$ (i.e., taking expectation over randomness in the trajectory).

By taking expectation on \mathcal{U}_k for both sides of Eq (2), we have,

$$\delta c_d \mathbb{E}_{\mathcal{U}_k} [\|\nabla f(\mathbf{x}_k)\|_2] \leq \mathbb{E}_{\mathcal{U}_k} [f(\mathbf{x}_k)] - \mathbb{E}_{\mathcal{U}_k} [\mathbb{E}_{\mathbf{u}_k \in \mathbb{S}} [f(\mathbf{x}_{k+1}) | \mathbf{x}_k]] + \frac{1}{2} L\delta^2 = \phi_k - \phi_{k+1} + L\delta^2 \quad (18)$$

By taking telescoping sum we have,

$$\sum_{k=1}^{K-1} \delta c_d \mathbb{E}_{\mathcal{U}_k} [\|\nabla f(\mathbf{x}_k)\|_2] \leq \phi_0 - \phi_{k+1} + \frac{1}{2} L \sum_{k=0}^{K-1} \delta^2 \leq f(\mathbf{x}_0) - f(\mathbf{x}^*) + \frac{1}{2} L \sum_{k=0}^{K-1} \delta^2 \quad (19)$$

So,

$$\min_k \mathbb{E} [\|\nabla f(\mathbf{x}_k)\|_2] \leq \frac{f(\mathbf{x}_0) - f(\mathbf{x}^*) + \frac{1}{2} L \sum_{k=0}^{K-1} \delta^2}{c_d \sum_{k=1}^{K-1} \delta} \quad (20)$$

in which $c_d = \frac{2\Gamma(\frac{d}{2})}{(d-1)\Gamma(\frac{d-1}{2})\sqrt{\pi}}$, so $\frac{1}{c_d} = O(\sqrt{d})$. By letting $\delta = \frac{1}{\sqrt{K}}$, we have $\min_k \mathbb{E} [\|\nabla f(\mathbf{x}_k)\|_2] = O(\frac{\sqrt{d}}{\sqrt{K}})$. \square

Proof of Theorem 2. According to Proposition 1, under Assumption 1,

$$\delta c_d \|\nabla f(\mathbf{x}_k)\|_2 \leq f(\mathbf{x}_k) - \mathbb{E}_{\mathbf{u}_k \in \mathbb{S}} [f(\mathbf{x}_{k+1}) | \mathbf{x}_k] + \frac{1}{2} L\delta^2 \quad (21)$$

Under the convex assumption, we have:

$$f(\mathbf{x}_k) - f(\mathbf{x}^*) \leq \nabla f(\mathbf{x}_k)(\mathbf{x}_k - \mathbf{x}^*) \leq \|\nabla f(\mathbf{x}_k)\|_2 \|\mathbf{x}_k - \mathbf{x}^*\|_2 \leq R \|\nabla f(\mathbf{x}_k)\|_2 \quad (22)$$

Combining Eq (22) and Eq (21), we have:

$$\frac{\delta c_d}{R} (f(\mathbf{x}_k) - f(\mathbf{x}^*)) \leq f(\mathbf{x}_k) - \mathbb{E}_{\mathbf{u}_k \in \mathbb{S}} [f(\mathbf{x}_{k+1}) | \mathbf{x}_k] + \frac{1}{2} L\delta^2 \quad (23)$$

By taking expectation over \mathcal{U}_k on both sides, we have:

$$\frac{\delta c_d}{R}(\phi_k - f(\mathbf{x}^*)) \leq \phi_k - \phi_{k+1} + \frac{1}{2}L\delta^2 \quad (24)$$

By rearranging the above equation, we get:

$$\phi_{k+1} - f(\mathbf{x}^*) \leq (1 - \frac{\delta c_d}{R})(\phi_k - f(\mathbf{x}^*)) + \frac{1}{2}L\delta^2 \quad (25)$$

To simplify the notations, we define $\alpha = 1 - \frac{\delta c_d}{R} \in (0, 1)$, $r_k = \phi_k - f(\mathbf{x}^*)$. Then we have,

$$r_K \leq \alpha r_{K-1} + \frac{1}{2}L\delta^2 \leq \alpha^K r_0 + \frac{1}{2}L\delta^2 \sum_{j=0}^{K-1} \alpha^j \leq e^{-\frac{\delta c_d K}{R}} r_0 + \frac{L\delta^2}{2(1-\alpha)} = e^{-\frac{\delta c_d K}{R}} r_0 + \frac{L\delta R}{2c_d} \quad (26)$$

in which the last inequality is based on the fact that $\ln(1+x) < x$ when $x \in (-1, 1)$ and geometric series formula. \square

B. Proofs about Cost Analysis

Proof of Proposition 3. We prove by induction. Because of the low-cost initialization, we have $g(\mathbf{x}_0) \leq g(\tilde{\mathbf{x}}^*)$. Since $D \geq 0$, we naturally have $g(\mathbf{x}_0) \leq g(\tilde{\mathbf{x}}^*) + D$.

Next, let's assume $g(\mathbf{x}_k) \leq g(\tilde{\mathbf{x}}^*) + D$, we would like to prove $g(\mathbf{x}_{k+1}) \leq g(\tilde{\mathbf{x}}^*) + D$ also holds. We consider the following two cases,

(a) $g(\mathbf{x}_k) \leq g(\tilde{\mathbf{x}}^*)$; (b) $g(\tilde{\mathbf{x}}^*) < g(\mathbf{x}_k) \leq g(\tilde{\mathbf{x}}^*) + D$

In case (a), according to FLOW², $\mathbf{x}_{k+1} = \mathbf{x}_k + \delta \mathbf{u}_k$ or $\mathbf{x}_{k+1} = \mathbf{x}_k - \delta \mathbf{u}_k$, or $\mathbf{x}_{k+1} = \mathbf{x}_k$. Then according to the Lipschitz continuity in Assumption 2, we have $g(\mathbf{x}_{k+1}) \leq g(\mathbf{x}_k) + U \times z(\delta \mathbf{u}_k)$ or $g(\mathbf{x}_{k+1}) \leq g(\mathbf{x}_k) + U \times z(-\delta \mathbf{u}_k)$, or $g(\mathbf{x}_{k+1}) = g(\mathbf{x}_k)$. So we have $g(\mathbf{x}_{k+1}) \leq g(\mathbf{x}_k) + U \times \max_{\mathbf{u} \in \mathbb{S}} z(\delta \mathbf{u}) \leq g(\tilde{\mathbf{x}}^*) + U \times \max_{\mathbf{u} \in \mathbb{S}} z(\delta \mathbf{u}) = g(\tilde{\mathbf{x}}^*) + D$.

In case (b), where $g(\tilde{\mathbf{x}}^*) \leq g(\mathbf{x}_k) \leq g(\tilde{\mathbf{x}}^*) + D$, if $g(\mathbf{x}_{k+1}) \leq g(\tilde{\mathbf{x}}^*)$, then $g(\mathbf{x}_{k+1}) < g(\tilde{\mathbf{x}}^*) + D$ naturally holds; if $g(\mathbf{x}_{k+1}) > g(\tilde{\mathbf{x}}^*)$, we can prove $g(\mathbf{x}_{k+1}) < g(\mathbf{x}_k)$ by contradiction as follows.

Assume $g(\mathbf{x}_{k+1}) > g(\mathbf{x}_k)$. Since $g(\mathbf{x}_k) < g(\tilde{\mathbf{x}}^*) + D$, and $\mathbf{x}_{k+1} = \mathbf{x}_k + \delta \mathbf{u}_k$ or $\mathbf{x}_{k+1} = \mathbf{x}_k - \delta \mathbf{u}_k$, or $\mathbf{x}_{k+1} = \mathbf{x}_k$, we have $g(\mathbf{x}_{k+1}) < g(\mathbf{x}_k) + U \times \max_{\mathbf{u} \in \mathbb{S}} z(\delta \mathbf{u}) \leq g(\tilde{\mathbf{x}}^*) + 2U \times \max_{\mathbf{u} \in \mathbb{S}} z(\delta \mathbf{u})$. Thus we have $g(\tilde{\mathbf{x}}^*) < g(\mathbf{x}_k) < g(\mathbf{x}_{k+1}) \leq g(\tilde{\mathbf{x}}^*) + 2U \times \max_{\mathbf{u} \in \mathbb{S}} z(\delta \mathbf{u})$. Then based on Assumption 3, $f(\mathbf{x}_{k+1}) > f(\mathbf{x}_k)$. However, this contradicts to the execution of FLOW², in which $f(\mathbf{x}_{k+1}) \leq f(\mathbf{x}_k)$. Hence we prove $g(\mathbf{x}_k) \leq g(\tilde{\mathbf{x}}^*) + D$ \square

Proof of Theorem 3. According to Proposition 2, we have $g(\mathbf{x}_{k+1}) \leq D + g(\mathbf{x}_k)$, with $D = U \times \max_{\mathbf{u} \in \mathbb{S}} z(\delta \mathbf{u})$. When $k \leq \bar{k} = \lceil \frac{\gamma}{D} \rceil - 1$, we have $g(\mathbf{x}_k) \leq g(\mathbf{x}_0) + Dk \leq g(\mathbf{x}^*)$.

For $K^* \leq \bar{k}$,

$$\sum_{k=1}^{K^*} g(\mathbf{x}_k) \leq \sum_{k=1}^{K^*} (g(\mathbf{x}_0) + Dk) \leq \frac{K^*(g(\mathbf{x}_0) + g(\tilde{\mathbf{x}}^*))}{2} \quad (27)$$

For $K^* > \bar{k}$,

$$\begin{aligned}
 \sum_{k=1}^{K^*} g(\mathbf{x}_k) &= \sum_{k=1}^{\bar{k}} g(\mathbf{x}_k) + \sum_{k=\bar{k}+1}^{K^*} g(\mathbf{x}_k) \leq \sum_{k=1}^{\bar{k}} (g(\mathbf{x}_0) + Dk) + \sum_{k=\bar{k}+1}^{K^*} (g(\tilde{\mathbf{x}}^*) + D) \\
 &\leq \bar{k}g(\mathbf{x}_0) + \frac{1}{2}D\bar{k}(1+\bar{k}) + (K^* - \bar{k})(g(\tilde{\mathbf{x}}^*) + D) \\
 &\leq \bar{k}(g(\tilde{\mathbf{x}}^*) - D\frac{(\bar{k}-1)}{2}) + (K^* - \bar{k})(g(\tilde{\mathbf{x}}^*) + D) \\
 &= K^*g(\tilde{\mathbf{x}}^*) + D(K^* - \frac{\bar{k}(\bar{k}+1)}{2}) \\
 &\leq K^*g(\tilde{\mathbf{x}}^*) + DK^* - \frac{(\gamma/D-1)\gamma}{2}
 \end{aligned} \tag{28}$$

In each iteration k , FLOW² requires the evaluation of configuration $\mathbf{x}_k + \delta\mathbf{u}$ and may involve the evaluation of configuration $\mathbf{x}_k - \delta\mathbf{u}$. Thus, $t_k \leq g(\mathbf{x}_k + \delta\mathbf{u}) + g(\mathbf{x}_k - \delta\mathbf{u}) \leq 2(g(\mathbf{x}_k) + D)$. Then we have

$$T \leq 2 \sum_{k=1}^{K^*} (g(\mathbf{x}_k) + D) = 2 \sum_{k=1}^{K^*} g(\mathbf{x}_k) + 2K^*D \tag{29}$$

Substituting Eq (27) and Eq (28) into Eq (29) respectively finishes the proof. \square

Proof of Proposition 5. We prove by induction similar to the proof of Proposition 3. Since the first point x_0 in FLOW² is initialized in the low-cost region, $g(\mathbf{x}_0) \leq g(\tilde{\mathbf{x}}^*)$. So $g(\mathbf{x}_0) \leq g(\tilde{\mathbf{x}}^*)C$ holds based on Fact 1. Next, let us assume $g(\mathbf{x}_k) \leq g(\tilde{\mathbf{x}}^*)C$, and we would like to prove $g(\mathbf{x}_{k+1}) \leq g(\tilde{\mathbf{x}}^*)C$. We consider the following two cases:

(a) $g(\mathbf{x}_k) \leq g(\tilde{\mathbf{x}}^*)$; (b) $g(\tilde{\mathbf{x}}^*) < g(\mathbf{x}_k) \leq g(\tilde{\mathbf{x}}^*)C$

In case (a), according to FLOW², $\mathbf{x}_{k+1} = \mathbf{x}_k + \delta\mathbf{u}_k$ or $\mathbf{x}_{k+1} = \mathbf{x}_k - \delta\mathbf{u}_k$ or $\mathbf{x}_{k+1} = \mathbf{x}_k$. Accordingly, $g(\mathbf{x}_{k+1}) = g(\mathbf{x}_k)c(\delta\mathbf{u}_k)$ or $g(\mathbf{x}_{k+1}) = g(\mathbf{x}_k)c(-\delta\mathbf{u}_k)$ or $g(\mathbf{x}_{k+1}) = g(\mathbf{x}_k)$ based on the fact Fact 1, so we have $g(\mathbf{x}_{k+1}) \leq g(\mathbf{x}_k) \max_{\mathbf{u} \in \mathbb{S}} c(\delta\mathbf{u}) \leq g(\tilde{\mathbf{x}}^*) \max_{\mathbf{u} \in \mathbb{S}} c(\delta\mathbf{u}) = g(\tilde{\mathbf{x}}^*)C$.

In case (b), where $g(\tilde{\mathbf{x}}^*) < g(\mathbf{x}_k) \leq g(\tilde{\mathbf{x}}^*) \max_{\mathbf{u} \in \mathbb{S}} c(\delta\mathbf{u})$, if $g(\mathbf{x}_{k+1}) \leq g(\tilde{\mathbf{x}}^*)$, then $g(\mathbf{x}_{k+1}) \leq \max_{\mathbf{u} \in \mathbb{S}} g(\tilde{\mathbf{x}}^* + \delta\mathbf{u})$ follows; if $g(\mathbf{x}_{k+1}) > g(\tilde{\mathbf{x}}^*)$, we can prove $g(\mathbf{x}_{k+1}) \leq g(\mathbf{x}_k)$ by contradiction as follows.

Assume $g(\mathbf{x}_{k+1}) > g(\mathbf{x}_k)$. Since $g(\mathbf{x}_k) \leq \max_{\mathbf{u} \in \mathbb{S}} g(\tilde{\mathbf{x}}^* + \delta\mathbf{u})$, and $\mathbf{x}_{k+1} = \mathbf{x}_k + \delta\mathbf{u}_k$ or $\mathbf{x}_{k+1} = \mathbf{x}_k - \delta\mathbf{u}_k$ or $\mathbf{x}_{k+1} = \mathbf{x}_k$, we have $g(\mathbf{x}_{k+1}) \leq g(\mathbf{x}_k) \max_{\mathbf{u} \in \mathbb{S}} c(\delta\mathbf{u}) \leq g(\tilde{\mathbf{x}}^*)(\max_{\mathbf{u} \in \mathbb{S}} c(\delta\mathbf{u}))^2 = g(\tilde{\mathbf{x}}^*)C^2$. Thus, we have $g(\tilde{\mathbf{x}}^*)C^2 > g(\mathbf{x}_{k+1}) > g(\mathbf{x}_k) > g(\tilde{\mathbf{x}}^*)$, and then based on Assumption 5, we have $f(\mathbf{x}_{k+1}) > f(\mathbf{x}_k)$. However, this contradicts to the execution of FLOW², in which $f(\mathbf{x}_{k+1}) \leq f(\mathbf{x}_k)$. Hence, we prove $g(\mathbf{x}_{k+1}) < g(\mathbf{x}_k) \leq g(\tilde{\mathbf{x}}^*)C$. \square

Proof of Theorem 4. According to Proposition 4, we have $g(\mathbf{x}_{k+1}) \leq Cg(\mathbf{x}_k)$, with $C = \max_{\mathbf{u} \in \mathbb{S}} c(\delta\mathbf{u})$.

When $k \leq \bar{k} = \lceil \frac{\log \gamma}{\log C} \rceil - 1$, we have $g(\mathbf{x}_k) \leq C^k g(\mathbf{x}_0) \leq g(\mathbf{x}^*)$.

For $K^* > \bar{k}$,

$$\begin{aligned}
 \sum_{k=1}^{K^*} g(\mathbf{x}_k) &= \sum_{k=1}^{\bar{k}} g(\mathbf{x}_k) + \sum_{k=\bar{k}+1}^{K^*} g(\mathbf{x}_k) \leq \sum_{k=1}^{\bar{k}} g(\mathbf{x}_0)C^k + \sum_{k=\bar{k}+1}^{K^*} g(\tilde{\mathbf{x}}^*)C \leq \frac{g(\tilde{\mathbf{x}}^*) - g(\mathbf{x}_0)}{C-1} + (K^* - \bar{k})g(\tilde{\mathbf{x}}^*)C \quad (30) \\
 &= g(\tilde{\mathbf{x}}^*)\left(\frac{\gamma-1}{\gamma(C-1)} + (K^* - \bar{k})C\right) \\
 &= g(\tilde{\mathbf{x}}^*)\left(K^*C + \frac{\gamma-1}{\gamma(C-1)} - \frac{\log \gamma}{\log C}C + C\right)
 \end{aligned}$$

Similar to the proof of Proposition 3, in each iteration k , $t_k \leq g(\mathbf{x}_k + \delta\mathbf{u}) + g(\mathbf{x}_k - \delta\mathbf{u}) \leq 2g(\mathbf{x}_k)C$. Then we have

$$T \leq 2C \sum_{k=1}^{K^*} g(\mathbf{x}_k) \leq g(\tilde{\mathbf{x}}^*) \cdot 2C \left(K^*C + \frac{\gamma-1}{\gamma(C-1)} - \frac{\log \gamma}{\log C}C + C \right) \quad (31)$$

For $K^* \leq \bar{k}$, $\sum_{k=1}^{K^*} g(\mathbf{x}_k) \leq \sum_{k=1}^{\bar{k}} g(\mathbf{x}_k)$, and the bound on T is obvious from Eq (30) and (31). \square

C. More Details about CEO and Experiments

C.1. More details about CEO

Our HPO solution CEO is presented in Algorithm 2. We explain several design choices made in Algorithm 2 as follows.

- The setting of no improvement threshold N : in CEO, we set $N = 2^{d-1}$. At point \mathbf{x}_k , define $\mathbf{U} = \{\mathbf{u} \in \mathbb{S} | \text{sign}(\mathbf{u}) = \text{sign}(\nabla f(\mathbf{x}_k))\}$, if $\nabla f(\mathbf{x}_k) \neq \mathbf{0}$, i.e., \mathbf{x}_k is not a first-order stationary point, $\forall \mathbf{u} \in \mathbf{U}$, $f'_{\mathbf{u}}(\mathbf{x}_k) = \nabla f(\mathbf{x}_k)^T \mathbf{u} > 0$, and $f'_{-\mathbf{u}}(\mathbf{x}_k) < 0$. Even when L-smoothness is only satisfied in $\mathbf{U} \cup -\mathbf{U}$, we will observe a decrease in loss when $\mathbf{u} \in \mathbf{U} \cup -\mathbf{U}$. The probability of sampling such \mathbf{u} is $\frac{2}{2^d}$. It means that we are expected to observe a decrease in loss after 2^{d-1} iterations even in this limited smoothness case.
- Initialization and lower bound of the stepsize: we consider the optimization iterations between two consecutive resets as one *round* of FLOW². At the beginning of each round r , δ_k is initialized to be a constant that is related to the round number: $\delta_k = r \log 2 + \delta_1$ with $\delta_1 = \sqrt{d'} \log 2$. Let δ_{lower} denotes the lower bound on the stepsize. It is computed according to the minimal gap required on the change of each hyperparameter. For example, if a hyperparameter is an integer type, the required minimal gap is 1. When no such requirement is posed, we set δ_{lower} to be a small value $0.01 \log 2$.
- Projection function: as we mentioned in the main content of the paper, the newly proposed configuration $\mathbf{x}_k \pm \mathbf{u}_k$ is not necessarily in the feasible hyperparameter space. To deal with such scenarios, we use a projection function $\text{Proj}_{\mathcal{X}}(\cdot)$ to map the proposed new configuration \mathbf{x}_{k+1} to the feasible space. In CEO, the following projection function is used $\text{Proj}_{\mathcal{X}}(\mathbf{x}') = \arg \min_{\mathbf{x} \in \mathcal{X}} \|\mathbf{x} - \mathbf{x}'\|_1$ (in line 6 of Algorithm 2), which is a straightforward way to handle discrete hyperparameters and bounded hyperparameters. After the projection operation, if the loss function is still non-differentiable with respect to \mathbf{x} , smoothing techniques such as Gaussian smoothing (Nesterov & Spokoiny, 2017), can be used to make it differentiable. And ideally, our algorithm can operate on the smoothed version of the original loss function, denoted as $\tilde{f}(\text{Proj}_{\mathcal{X}}(\mathbf{x}'))$. However, since the smoothing operation adds additional complexity to the algorithm and, in most cases, $\tilde{f}(\cdot)$ can be considered as a good enough approximation to $f(\cdot)$, the smoothing operation is omitted in our algorithm and implementation.

C.2. More details about experiments and results

The experiments are conducted in an E64is_v3 (Intel Xeon E5-2673 v4 @ 2.30GHz, 64 virtual CPUs, 432 GB memory) Azure Linux VM. For *Fashion-MNIST* and *riccardo*, we used two cores for each method (because these two datasets are

Algorithm 2 CEO

```

1: Inputs: 1. Feasible configuration space  $\mathcal{H}$ . 2. Initial low-cost configuration  $\mathbf{x}_0$ . 3. (Optional) Transformation function  $S, \tilde{S}$ .
2: Initialization: Initialize  $\mathbf{x}_0, \delta_1 = \sqrt{d'} \log 2$ . Set consecutively no improvement threshold  $N = 2^{d-1}, k' = 0, K_{\text{new}} = 0, l^{\text{r-best}} \leftarrow +\inf, r = 1$ 
3: for  $k = 1, 2, \dots$  do
4:   Sample  $\mathbf{u}_k$  uniformly at random from  $\mathbb{S}$ 
5:    $\mathbf{x}_k^+ \leftarrow \mathbf{x}_{k-1} + \delta_k \mathbf{u}_k, \mathbf{x}_k^- \leftarrow \mathbf{x}_{k-1} - \delta_k \mathbf{u}_k$ 
6:    $\mathbf{x}_k^+ \leftarrow \text{Proj}_{\mathcal{X}}(\mathbf{x}_k^+), \mathbf{x}_k^- \leftarrow \text{Proj}_{\mathcal{X}}(\mathbf{x}_k^-)$ 
7:   if  $f(\mathbf{x}_k^+) < f(\mathbf{x}_k)$  then
8:     Set  $\mathbf{x}_{k+1} \leftarrow \mathbf{x}_k^+$  and report  $\mathbf{x}_{k+1}$ 
9:   else
10:    if  $f(\mathbf{x}_k^-) < f(\mathbf{x}_k)$  then
11:      Set  $\mathbf{x}_{k+1} \leftarrow \mathbf{x}_k^-$  and report  $\mathbf{x}_{k+1}$ 
12:    else
13:       $\mathbf{x}_{k+1} \leftarrow \mathbf{x}_k, n \leftarrow n + 1$ 
14:      if  $f(\mathbf{x}_{k+1}) < l^{\text{r-best}}$  then
15:        Set  $l^{\text{r-best}} \leftarrow f(\mathbf{x}_{k+1}), k'' \leftarrow k$ 
16:      if  $n = N$  then
17:         $K_{\text{old}} \leftarrow k'' - k'$  if  $K_{\text{new}} = 0$ , else  $K_{\text{old}} \leftarrow K_{\text{new}}$ 
18:         $n \leftarrow 0, K_{\text{new}} \leftarrow k - k'$ 
19:        Set  $\delta_{k+1} \leftarrow \delta_k \sqrt{\frac{K_{\text{old}}}{K_{\text{new}}}}$ 
20:        if  $\delta_{k+1} \leq \delta_{\text{lower}}$  then
21:           $k' \leftarrow k, K_{\text{new}} \leftarrow k - k', l^{\text{r-best}} \leftarrow +\inf$ 
22:          Reset  $\mathbf{x}_{k+1} \leftarrow \mathbf{g}$ , where  $\mathbf{g} \sim N(\mathbf{x}_0, \mathbf{I})$ 
23:          Reset  $\delta_{k+1} \leftarrow r \log 2 + \delta_1$ 
24:           $r \leftarrow r + 1$ 
25:        else
26:          Set  $\delta_{k+1} \leftarrow \delta_k$ 

```

large and require more resources to converge to good hyperparameters). For all the other datasets, we used 1 core for each method. All the datasets are downloadable from openml.org. The openml task ids for each dataset are provided in Table 3.

We used the following libraries for baselines: HpBandSter 0.7.4 (<https://github.com/automl/HpBandSter>), BayesianOptimization 1.0.1 (<https://github.com/fmfn/BayesianOptimization>), and SMAC3 0.8.0 (<https://github.com/automl/SMAC3>).

EXPERIMENTS ON XGBOOST

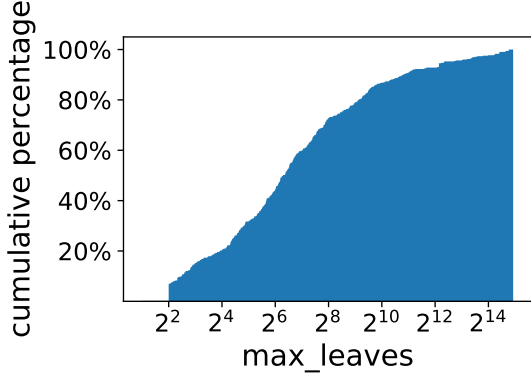
The 9 hyperparameters tuned in XGBoost in our experiment are listed in Table 2. Logarithm transformation is performed for all hyperparameters in CEO, CEO-0 and GP, for all hyperparameters except *colsample by level* and *colsample by tree* in SMAC and BOHB. The learning curves for all datasets are displayed in Figure 5.

The total evaluation cost of RS and BO-based methods can be largely affected by the setting of the cost-related hyperparameters' range. In this work, we used $\min(32768, \#\text{instance})$ as the upper bound of tree number and leaf number. To show that this range is not unnecessarily large, we visualize the distribution of these two hyperparameters in best configurations over all the datasets through a scatter plot in Figure 2. In this scatter plot, each point represents the best configurations of tree and leaf number found (among all the methods) on a particular dataset. This result shows that our settings of the upper bound of tree and leaf number are not unnecessarily large because we need to ensure that the configuration of the best models on all of the datasets can be covered by this range.

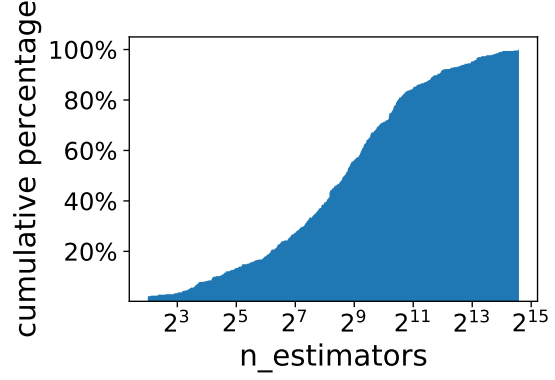
We compare the distribution of evaluation time for the best configuration found by each method (which also includes the computational time of that method at the corresponding iteration) in Figure 4. Since that CEO has the leading final performance on almost the all the datasets, we consider the best configuration found by CEO as the configuration that has

Table 2. Hyperparameters tuned in XGBoost

hyperparameter	type	range
tree num	int	[4, min(32768, # instance)]
leaf num	int	[4, min(32768, # instance)]
min child weight	float	[0.01, 20]
learning rate	float	[0.01, 0.1]
subsample	float	[0.6, 1.0]
reg alpha	float	[1e-10, 1.0]
reg lambda	float	[1e-10, 1.0]
colsample by level	float	[0.6, 1.0]
colsample by tree	float	[0.7, 1.0]



(a) cumulative histogram of max_leaves



(b) cumulative histogram of n_estimators

Figure 2. Distribution of two cost-related hyperparameters in best configurations over all the datasets

the appropriate complexity. From this figure we can observe that the best configurations found by BO methods tend to have unnecessarily large evaluation cost and CEO-0 tends to return configurations with insufficient complexity.

EXPERIMENTS ON DNN

The 5 hyperparameters tuned in DNN in our experiment are listed in Table 4. Table 5 shows the final loss and the cost used to reach that loss per method within two hours budget. Since experiments for DNN are more time consuming, we removed five large datasets comparing to the experiment for XGBoost, and all the results reported are averaged over 5 folds (instead of 10 as in XGBoost). The learning curves are displayed in Figure 6. In these experiments, CEO again has superior performance over all the compared baselines similar to the experiments for XGBoost.

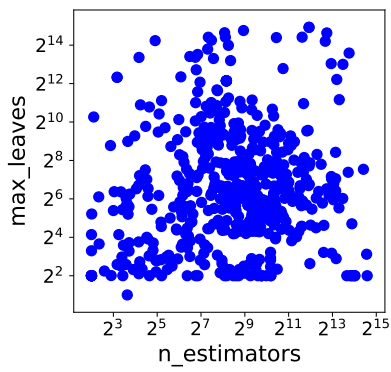


Figure 3. Scatter plot of two cost-related hyperparameters in best configurations over all the datasets

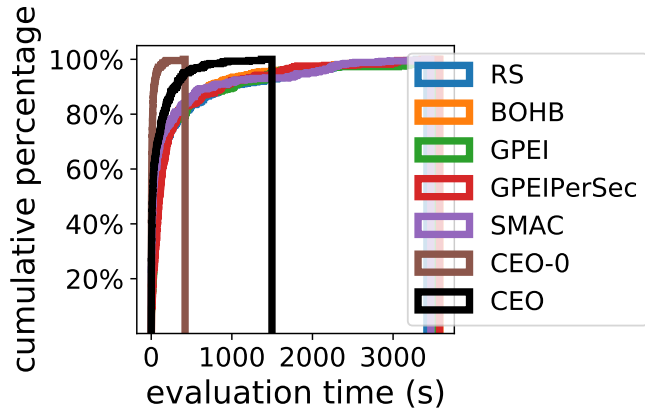


Figure 4. Distribution of evaluation time of the best XGBoost config found by each method

Table 3. Task ids on OpenML

dataset	id	dataset	id
adult	7592	Airlines	189354
Amazon_employee	34539	APSFailure	168868
Australian	146818	bank_marketing	14965
blood-transfusion	10101	car	146821
christine	168908	cnae-9	9981
connect-4	146195	credit-g	31
fabert	168852	Fashion-MNIST	146825
Helena	168329	higgs	146606
Jannis	168330	jasmine	168911
jungle_chess_2pcs	167119	kc1	3917
KDDCup09_appe	3945	kr-vs-kp	3
mfeat-factors	12	MiniBooNE	168335
nomao	9977	numerai28.6	167120
phoneme	9952	riccardo	178333
segment	146822	shuttle	146212
sylvine	168853	vehicle	53
volkert	168810		
bng_echomonths*	7323	bng_lowbwt*	7320
bng_breastTumor*	7324	bng_pbc*	7318
bng_pharynx*	7322	bng_pwLinear*	7325
fried*	4885	houses*	5165
house_8L*	2309	house_16H*	4893
mv*	4774	pol*	2292
poker*	10102	2dplane*	2306

Table 4. Hyperparameters tuned in DNN (fully connected Relu network with 2 hidden layers)

hyperparameter	type	range
neurons in first hidden layer	int	[4, 2048]
neurons in second hidden layer	int	[4, 2048]
batch size	int	[8, 128]
dropout rate	float	[0.2, 0.5]
learning rate	float	[1e-6, 1e-2]

Table 5. Optimality of score and cost for DNN tuning. The meaning of each cell in this table is the same as that in Table 1

Dataset	RS	BOHB	GPEI	GPEIPerSec	SMAC	CEO-0	CEO
adult	-20.8%	-0.2%	-32.0%	-47.6%	-2.2%	0.7072 (6670s)	-0.4%
Airlines	-21.2%	-1.9%	-42.0%	-40.6%	-11.3%	-10.5%	0.5663 (6613s)
Amazon.emp	-31.8%	-7.6%	-67.2%	-40.0%	-7.5%	-14.5%	0.2247 (7110s)
APSFailure	-0.8%	-0.9%	-0.4%	-1.2%	-0.8%	-0.3%	0.9963 (4639s)
Australian	-2.6%	0.8920 (7043s)	-3.5%	-3.3%	-2.2%	-7.7%	-0.5%
bank_marke	-63.1%	-5.5%	-9.5%	-7.2%	-5.3%	-2.8%	0.8085 (6128s)
blood-tran	-0.9%	-2.0%	-3.1%	-2.7%	-2.2%	1.4288 (4421s)	$\times 1.3$
car	-13.4%	-6.1%	-7.3%	-8.7%	-4.7%	-16.7%	0.6416 (6294s)
christine	-21.2%	-0.6%	-3.6%	-2.0%	-1.2%	-0.8%	0.9739 (3019s)
cnae-9	-0.4%	1.1148 (6192s)	-0.2%	-0.2%	-0.5%	-0.1%	$\times 1.1$
connect-4	-37.5%	-21.1%	-77.0%	-78.2%	-14.1%	-35.5%	0.5843 (7065s)
credit-g	-1.4%	-3.5%	-10.5%	-11.2%	-4.7%	0.7247 (2595s)	-2.5%
fabert	-1.1%	$\times 5.0$	-2.7%	-3.1%	-1.2%	-0.9%	1.0070 (1263s)
Helena	-58.0%	-30.7%	-42.0%	-56.1%	-27.1%	-26.7%	1.9203 (7191s)
higgs	-3.8%	-2.5%	-39.5%	-66.8%	-9.1%	-8.3%	0.6615 (5135s)
Jannis	-11.9%	-9.2%	-24.2%	-23.4%	-10.2%	-9.5%	0.7691 (6431s)
jasmine	-1.2%	0.8978 (4678s)	-2.1%	-2.0%	-1.8%	-1.3%	-0.4%
jungle_che	-14.8%	-32.9%	-23.9%	-37.4%	-14.0%	-35.7%	0.4403 (7013s)
kc1	-1.2%	-20.7%	-1.5%	-1.4%	-0.8%	0.8618 (6705s)	-0.4%
KDDCup09.a	-14.4%	-1.7%	-17.4%	-7.7%	0.3759 (6421s)	-3.9%	-0.5%
kr-vs-kp	-0.5%	-0.1%	-0.4%	-0.4%	-0.2%	-0.5%	0.9917 (3723s)
mfeat-fact	-5.6%	-1.7%	-2.8%	-3.2%	-2.2%	-3.9%	0.9739 (7182s)
MiniBooNE	-2.1%	-1.8%	-6.9%	-14.7%	-1.4%	-2.3%	0.9716 (7111s)
nomao	-0.8%	-0.2%	-1.3%	-2.1%	-0.6%	-0.5%	0.9839 (2039s)
numerai28.	-1.2%	-0.1%	-25.7%	-29.0%	-5.4%	-4.3%	1.3909 (6676s)
phoneme	-1.3%	-0.7%	-0.1%	-0.1%	-0.6%	-1.1%	0.9016 (3842s)
segment	-3.9%	-0.1%	-3.6%	-1.9%	-2.2%	-3.7%	0.9088 (3301s)
shuttle	-27.9%	-16.1%	-23.4%	-52.1%	-26.8%	-28.1%	0.8719 (4657s)
sylvine	-7.0%	-6.4%	-8.3%	-6.0%	-1.8%	-11.1%	0.7935 (4733s)
vehicle	-8.0%	-24.8%	-8.9%	-7.9%	-2.1%	-18.4%	0.3195 (6830s)
volkert	-16.3%	-11.2%	-27.1%	-21.9%	-7.1%	-14.4%	0.8716 (7111s)
2dplanes*	-21.4%	-1.5%	-1.7%	-1.2%	-1.3%	-2.6%	0.9357 (6321s)
bng_breast*	-5.3%	-2.7%	-11.2%	-6.7%	-0.6%	-13.0%	0.0739 (6170s)
bng_ecomo*	-1.6%	-0.4%	-0.4%	-1.0%	-1.0%	-1.2%	0.4252 (2859s)
bng_lowbwt*	-3.9%	-0.5%	-1.7%	-4.4%	-2.8%	-11.9%	0.5631 (4625s)
bng_pwLine*	-3.0%	-20.9%	-3.8%	-11.9%	-2.1%	-4.0%	0.6005 (4524s)
fried*	-24.8%	-8.1%	-21.1%	-19.8%	-15.0%	-25.2%	0.6383 (6404s)
house_16H*	-6.0%	-2.6%	-4.4%	-4.6%	-3.8%	-16.2%	0.1678 (6410s)
house_8L*	-3.8%	-1.3%	-8.4%	-0.2%	-1.5%	-15.5%	0.1424 (6487s)
houses*	-24.8%	-16.6%	-27.8%	-1.1%	-15.5%	-45.9%	0.2146 (6109s)
mv*	-11.4%	-8.9%	-22.8%	-11.0%	-9.3%	-7.3%	0.8856 (4887s)
pol*	-14.8%	-2.8%	-4.1%	-12.6%	-11.3%	0.6860 (4736s)	-0.7%

* for regression datasets

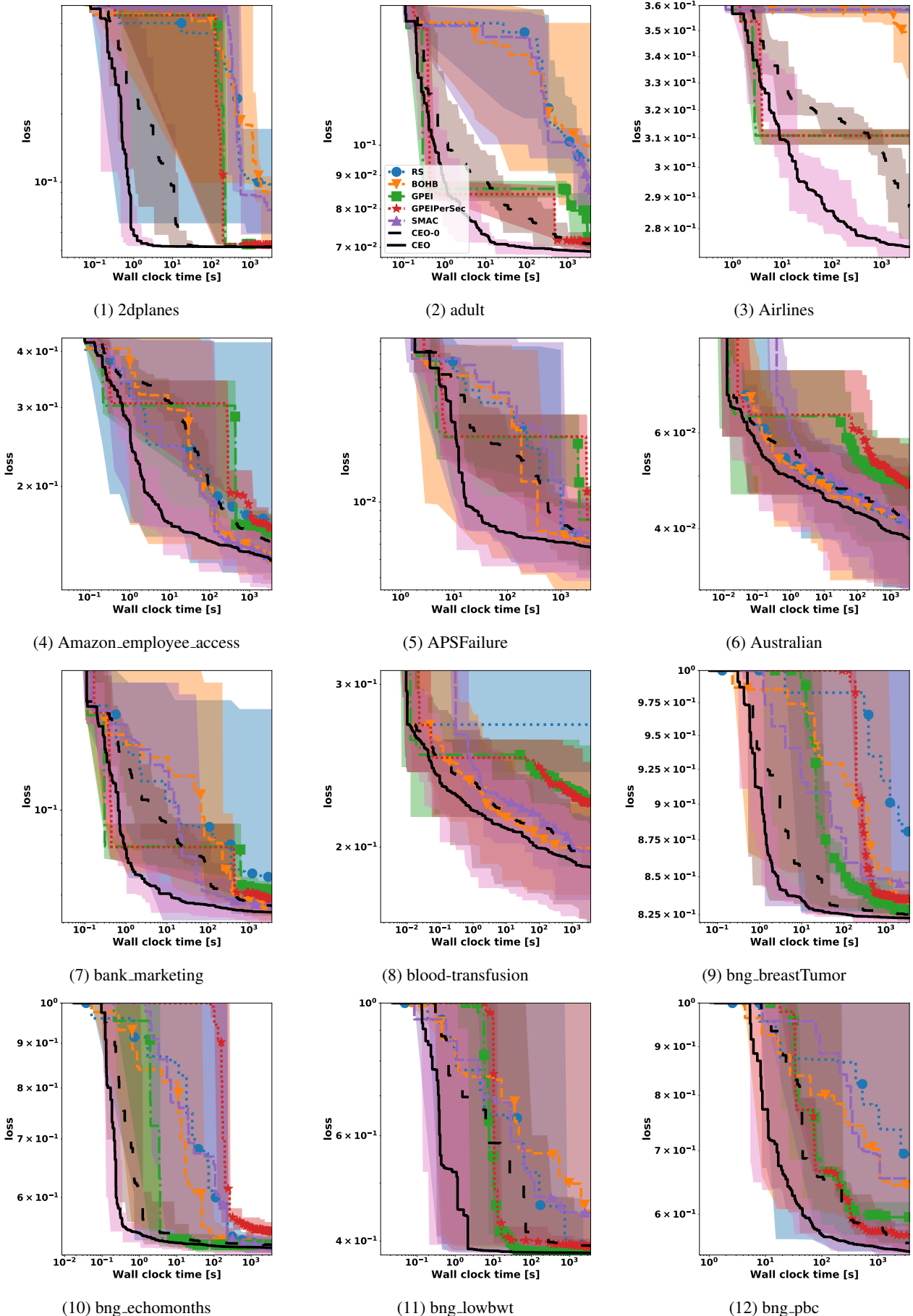


Figure 5. Optimization performance curve for XGBoost (pt 1/4)

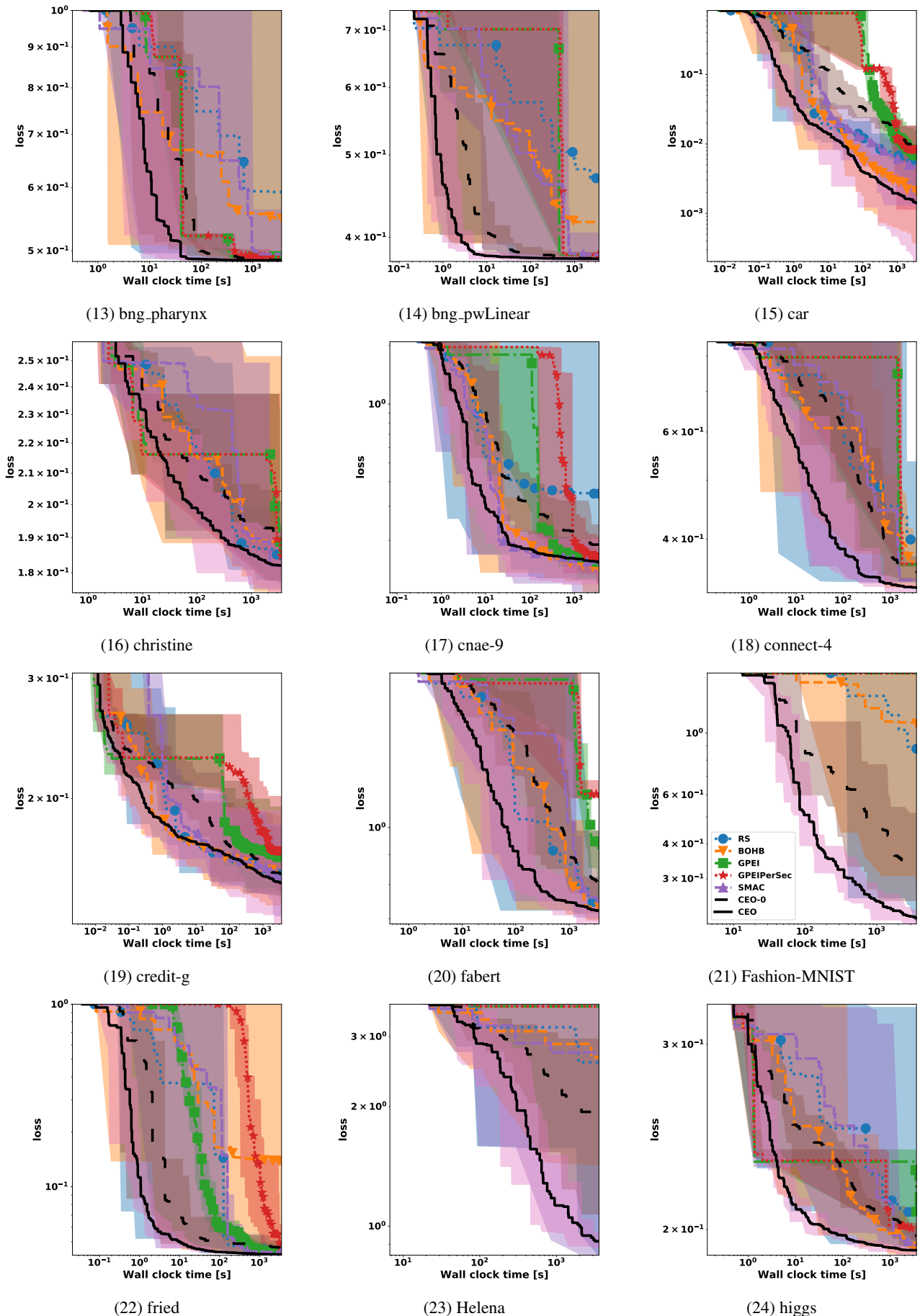


Figure 5. Optimization performance curve for XGBoost (pt 2/4)

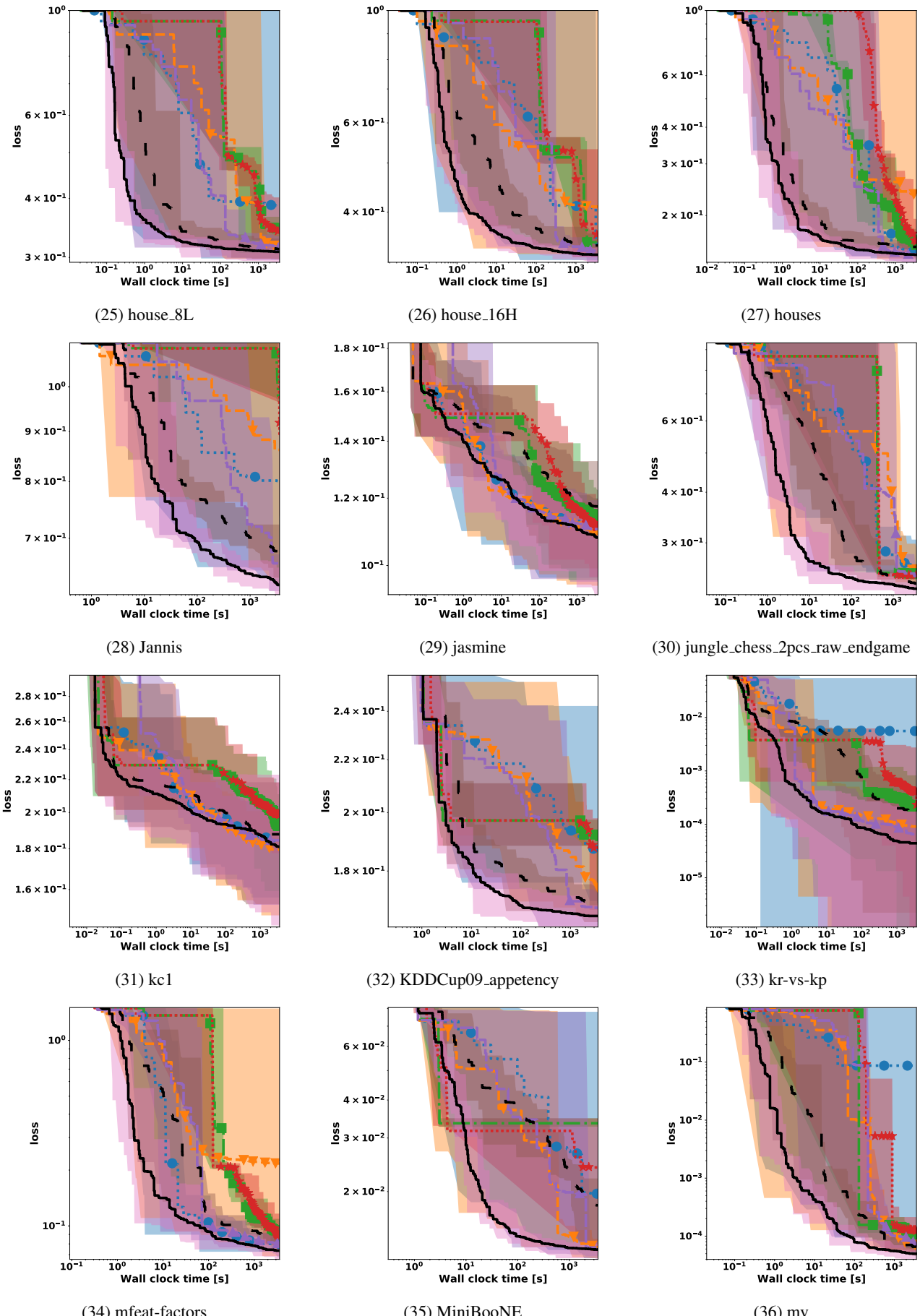


Figure 5. Optimization performance curve for XGBoost (pt 3/4)

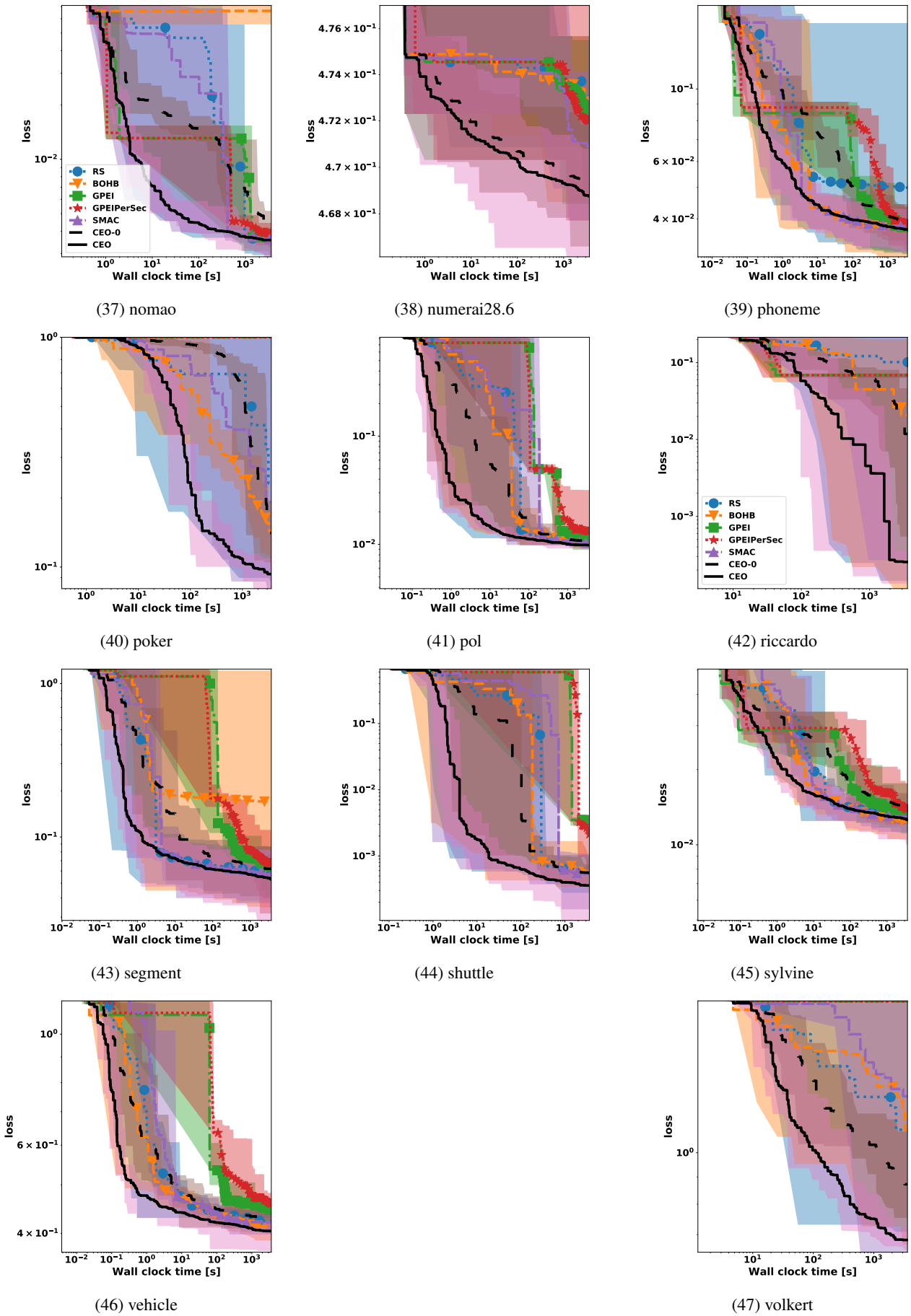


Figure 5. Optimization performance curve for XGBoost (pt 4/4)

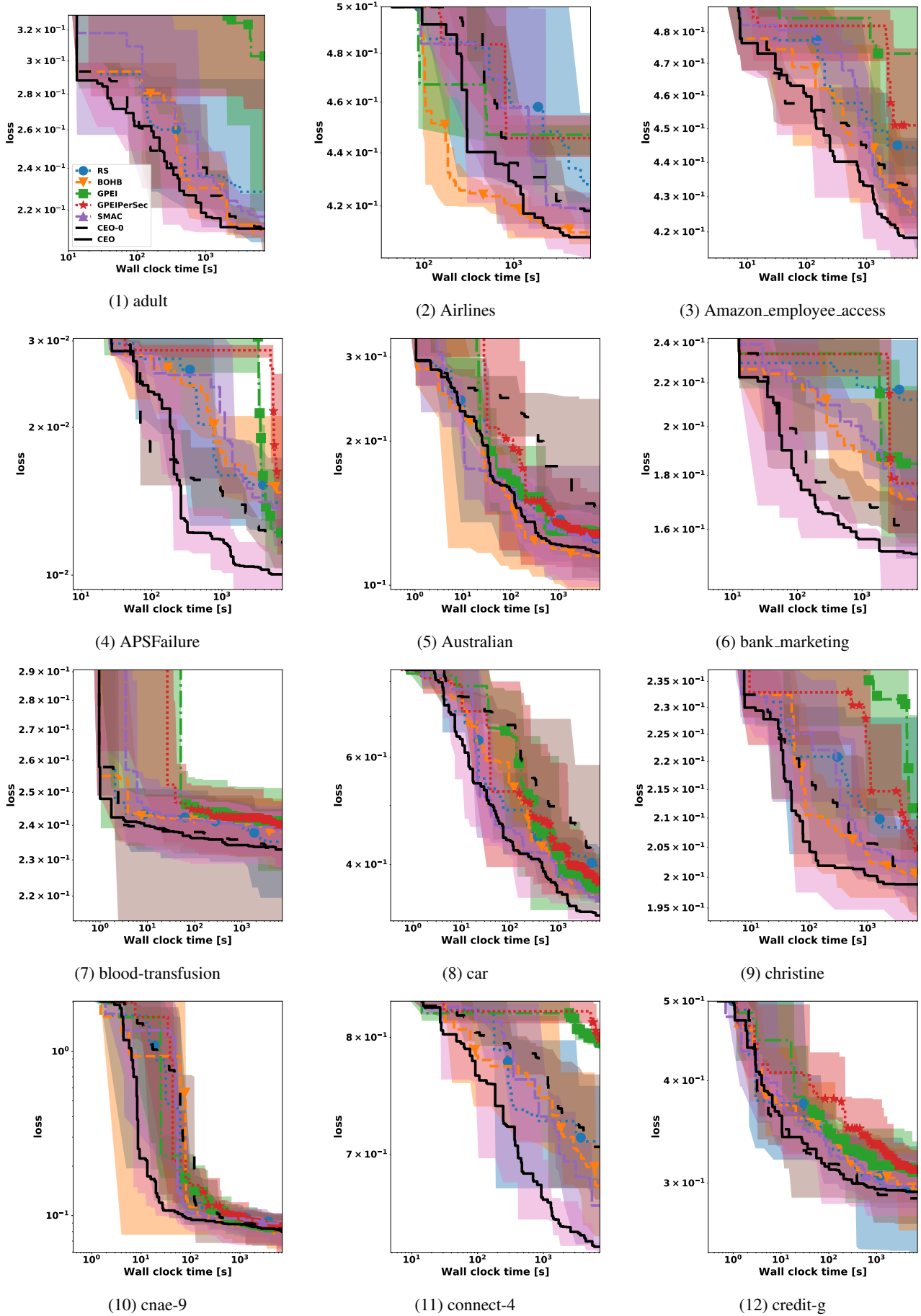


Figure 6. Optimization performance curve for DNN (pt 1/4)

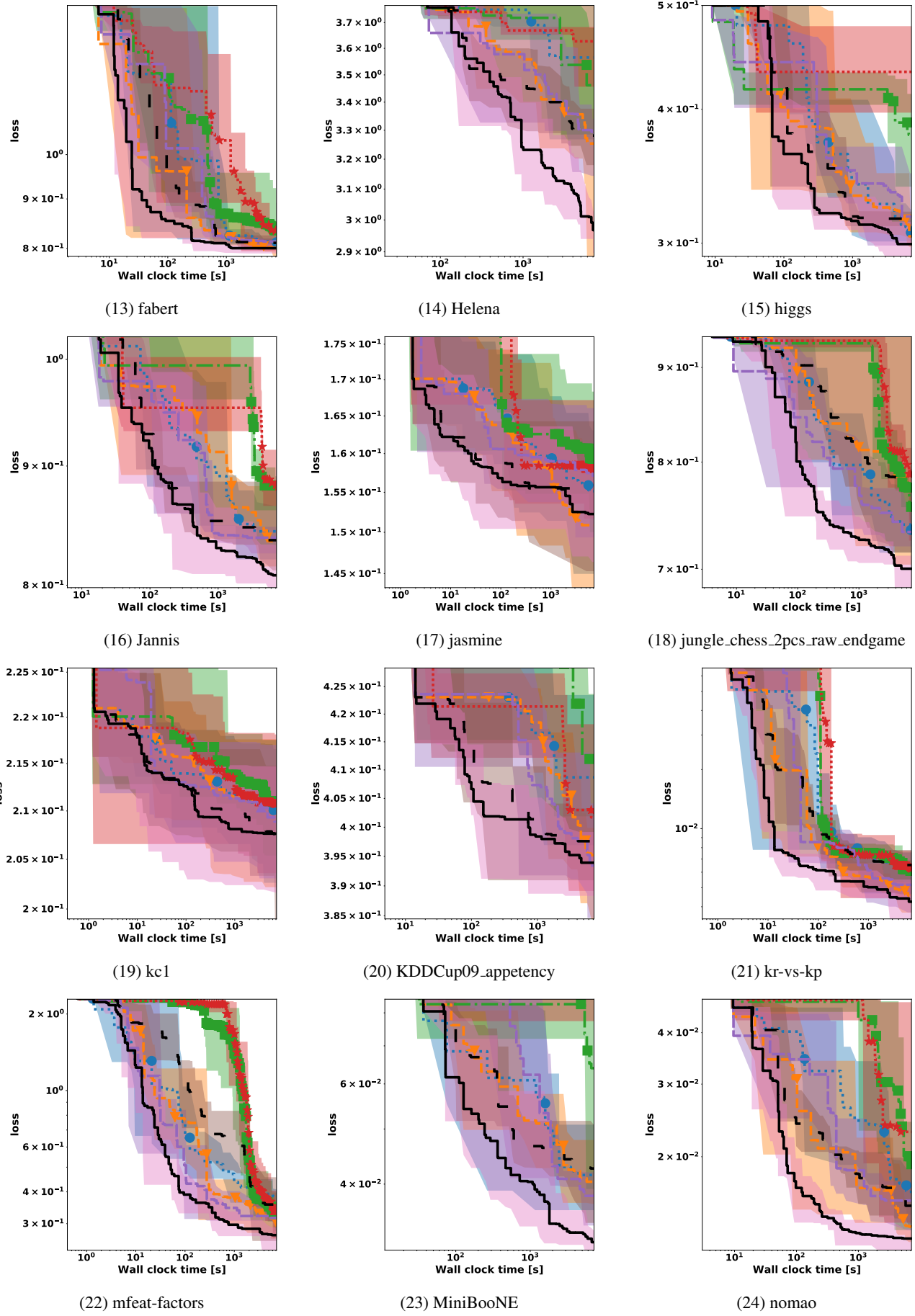


Figure 6. Optimization performance curve for DNN (pt 2/4)

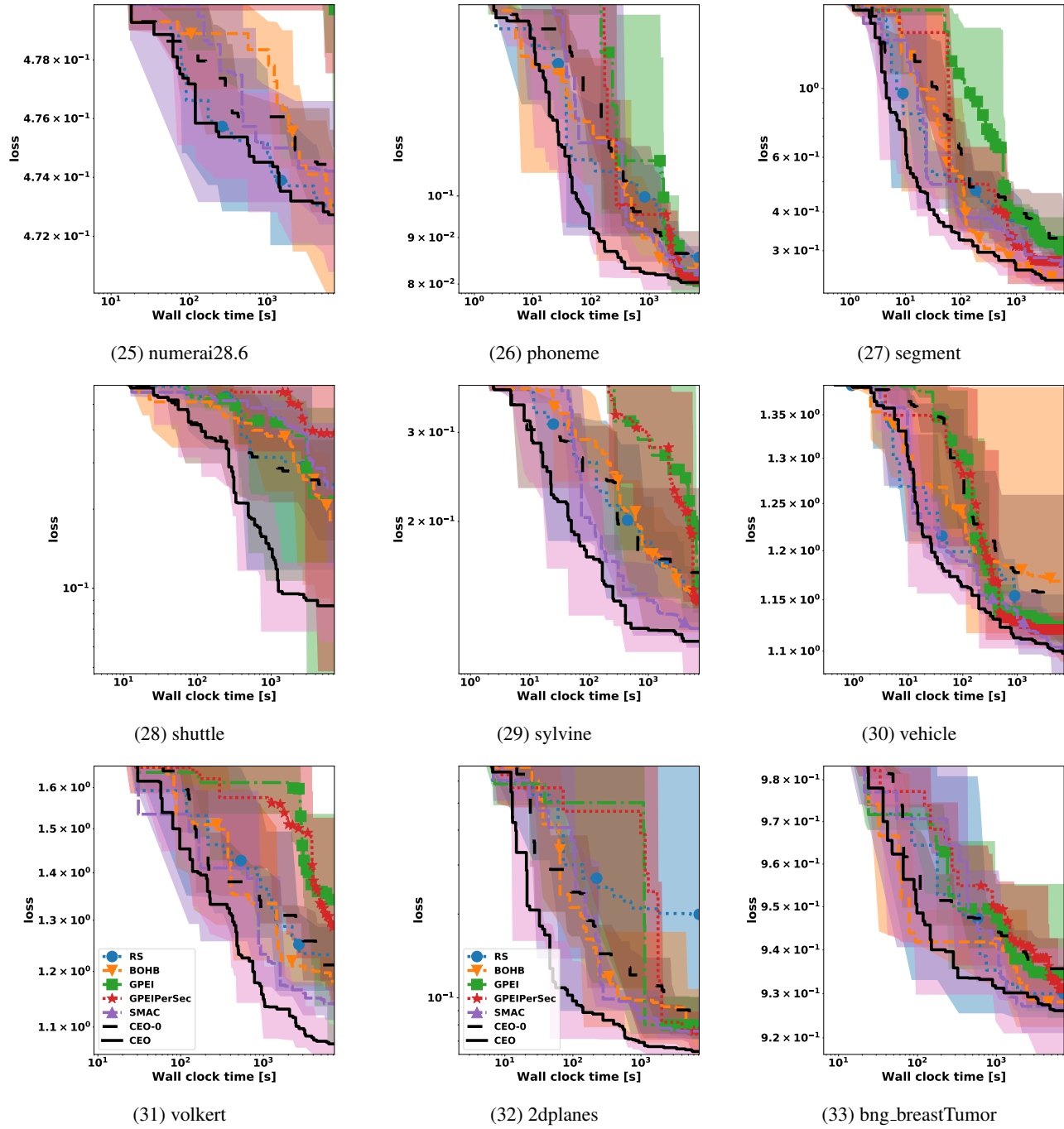


Figure 6. Optimization performance curve for DNN (pt 3/4)

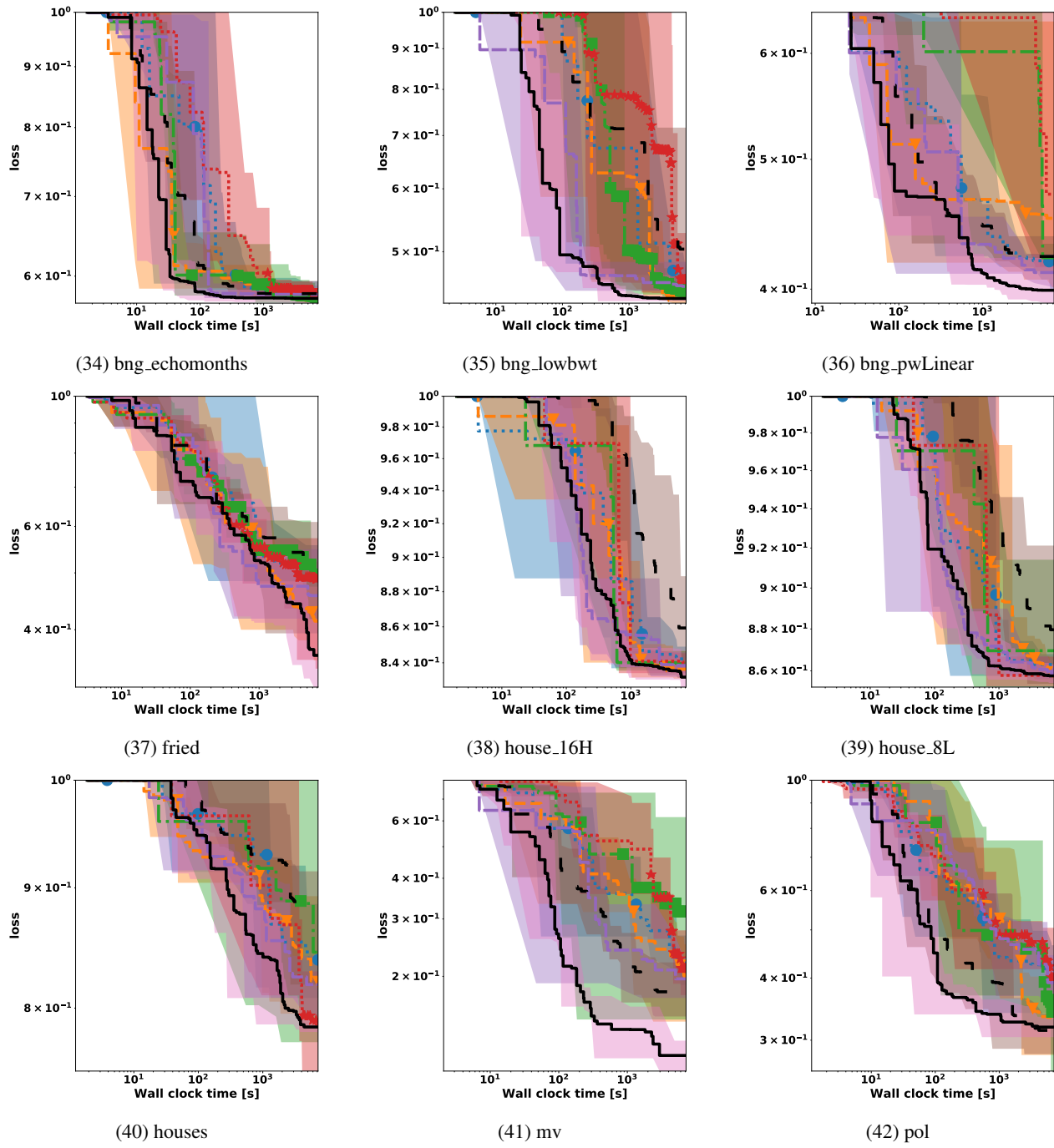


Figure 6. Optimization performance curve for DNN (pt 4/4)